

**INVESTIGATING TRIPLEX-FORMING OLIGONUCLEOTIDES THAT  
TARGET THE MOUSE *Cd9* GENE**

by  
Benedicta Asamoah

A thesis submitted to Johns Hopkins University in conformity with  
the requirements for the degree of Master of Science

Baltimore, Maryland  
October, 2013

## Abstract

### Background

Mammalian oocyte research has benefited from gene manipulation tools such as homologous recombination, antisense and RNA interference, with limitations. Triplex-forming oligonucleotides (TFOs) can modulate gene expression in a sequence specific manner. Their ability to directly target the gene makes them attractive as genome manipulation tools. The goal of this thesis project was to investigate the possibility of using TFOs to inhibit expression of genes that are important for the maturation or fertilization of oocytes in a mouse cell culture model system.

### Materials and methods

We used a web-based search engine to identify TFO binding sites in *Cd9*, *Plk1* and *Cdcd25b* genes and selected some sequences for studies. We used biochemical, and cell biology approaches such as UV thermal denaturation, electrophoretic mobility shift assays, live cell fluorescence microscopy, RT-qPCR and western blot techniques to investigate the in vitro characteristics and in vivo activity of the TFOs.

### Results

Only a small subset of the *Cd9*, *Plk1* and *Cdc25b* deoxyribo-TFOs tested formed stable triplexes with their target DNA duplexes. 2'-OMe TFOs formed more stable triplexes and 2'-OMe-Pt-TFOs cross-linked with higher efficiencies than their deoxyribo counterparts. FITC-labeled *Cd9* T2 3' Pt-TFO complexed to transfection reagents FuGENE HD or Lipofectamine™ 2000 had different uptake efficiencies and sub-cellular distribution. RT-qPCR analyses of mRNA extracted from cells treated with a Lipofectamine™

2000/FITC-labeled *Cd9* T2 3' Pt-TFO complex showed a 32% decrease in the *Cd9* mRNA level. However a similar decrease was observed when the cells were transfected with a Lipofectamine<sup>TM</sup> 2000/FITC-labeled scrambled 3' Pt-TFO. No change in CD9 protein levels was observed for either FITC-labeled scrambled or *Cd9* 3' Pt-TFO complexed to Lipofectamine<sup>TM</sup> 2000 or FuGENE HD.

### **Conclusion**

2'-O-methylribo modification increases the stability of the triplexes formed by TFOs and the efficiency of cross-linking by Pt-TFOs. Our results indicate that uptake efficiency and nuclear localization differs for different transfection reagents and determines the in vivo activity of the Pt-TFO. Although the FITC-labeled *Cd9* T2 3' Pt-TFO demonstrated modest ability to inhibit the *Cd9* mRNA levels we were unable to demonstrate that this inhibition was a sequence specific effect of the TFO.

## **Acknowledgement**

I would like to thank Drs. Randy Bryant, Dr. Paul Miller, Dr. Janice Evans, Dr. Haung, and the whole BMB department for enriching my life and providing guidance when I needed it the most. I appreciate the opportunities given to me by the Miller and Janice Lab's to perform my master's thesis. The thesis project has been an invaluable experience that has allowed me to develop critical thinking and research skills that will be invaluable to my future pursuant in the research field. My sincere gratitude to my principal investigators, advisors, and thesis readers Drs. Paul Miller and Janice Evans. They have been tremendous mentors, whose invaluable inputs have enriched my academic research experience.

I'm indebted to Mindy Graham for her patience, her kindness, and emotional support throughout the past year. She taught me everything I know and then some. I've grown to know her as a great colleague but I'm even more appreciative of the invaluable friend she's become. To past and present Miller and Janice lab members, including Java, Lauren M, Lauren, Hyo, Abby, Katherine and Grace, thank you all for your support and help during the research. To everyone in Pierre and Fengyi's Lab, I say thanks. I'm grateful for taking time out of your schedule to provide help with research protocols and donate materials.

My deepest gratitude to my parents, Reynolds and Grace Asamoah for supporting my career goals with their constant encouragement and motivation. My love and thanks to my brothers, Michael, Justin and Kevin, whose constant admiration motivates my daily endeavors. Last but not least, I would like to thank all my friends, new and old ones, you have all been instrumental in my success and I remain grateful.

## Table of Contents

Abstract .....	ii
Acknowledgements .....	iv
Table of Contents .....	v
List of Tables .....	vi
List of Figures .....	vii
Acronyms.....	viii
Literature Review.....	1
Materials and Methods .....	20
Results.....	31
Discussion.....	45
References .....	88
Curriculum Vitae.....	106

## List of Tables

<b>Table 1</b> - The sequences of oligonucleotides and DNA duplexes .....	62
<b>Table 2</b> - Melting temperature and electron mobility shift assay (cross-linking) of 2'- 0-methylribonucleotides <i>Cd9</i> T2 3' and 5' TFO .....	64
<b>Table 3</b> - Primer sequences used in RT-qPCR.....	65

## List of Figure

<b>Figure 1</b> – Characteristics of TFOs .....	66
<b>Figure 2</b> – General representation of the thermal denaturation curve and the melting temperatures of all deoxyribonucleotides TFO .....	68
<b>Figure 3</b> - Platinated structure of TFO.....	70
<b>Figure 4</b> - General representation of an electron mobility shift assay and results of the cross-linking for deoxyribonucleotides.....	72
<b>Figure 5</b> - Schematic representation of the <i>Cd9</i> target and the structural features of CD9 protein .....	74
<b>Figure 6</b> - General thermal denaturation curve of 2'-0-methylribonucleotide triplex....	76
<b>Figure 7</b> - Melting temperature and electrophoretic mobility shift assay (cross-linking) of <i>Cd9</i> T2 3' TFO and FITC-labeled <i>Cd9</i> T2 3' and Scrambled 3' TFO.....	78
<b>Figure 8</b> - Cellular uptake and transfection efficiency: FuGENE vs. Lipofectamine transfection reagent .....	80
<b>Figure 9</b> - RT-qPCR standard curve.....	82
<b>Figure 10</b> - RT-qPCR: FuGENE vs. Lipofectamine transfection reagent.....	84
<b>Figure 11</b> - Western Blot: FuGENE vs. Lipofectamine transfection reagent.....	86

## Acronyms

TFO	triplex-forming oligonucleotide
Pt-TFO oligonucleotide	active platinated triplex forming
Inert Pt-TFO oligonucleotide	inactive platinated triplex forming
2'-OMe	2'-O-methylribose
Cd9	<i>Cd9</i> gene
CD9	CD9 protein
m <i>Cd9</i>	mouse <i>Cd9</i> primer
m <i>Gapdh</i>	mouse <i>Gapdh</i> primer
<i>Gapdh</i>	glyceraldehyde-3-phosphate dehydrogenase
<i>Plk1</i>	polo like kinase 1 gene
<i>Cdc25b</i>	cell division cycle 25 b gene
EMSA	electron mobility shift assay
FITC	6-carboxyfluorescein



## **LITERATURE REVIEW**

### **1. Introduction**

Gene modulation technologies in biomedical research have facilitated the discovery of the functions of specific gene products, including their molecular mechanisms in a myriad of biological processes. These insights have far-reaching implications in basic science, and in clinical and therapeutic research. In research of mammalian oocytes, genetic manipulations have provided significant insights into genes involved in processes such as cell cycle division, proliferation differentiation, and fertilization (Kaji et al., 2000; Lindqvist, Källström, & Karlsson Rosenthal, 2004). These studies and their outputs are of considerable interest due to their applications for human reproductive health.

Traditionally, homologous recombination techniques have been used to generate knockout mice for studies to deduce gene function (Miyado et al., 2000; Torgasheva, Rubtsov, & Borodin, 2013). While efficient, this method is time and labor-intensive. Arguably, the Knockout Mouse Project provides significant access to a wide collection of mouse knockouts and embryonic stem cells (Austin et al., 2004) or mouse knockouts can be obtained from commercial resources. However, preparation of knockout mice can result in unpredicted phenotypes, which coupled with the high cost of production necessitates the need for additional efforts to achieve desired phenotypes (Austin et al., 2004). Recently, different approaches including antisense oligonucleotides and RNA interference (RNAi) have emerged as genetic

manipulation tools useful for studying gene function in mammalian oocytes (Dias & Stein, 2002; Sarnova, Malik, Sedlacek, & Svoboda, 2010).

Antisense oligonucleotides are single-stranded oligonucleotides targeting specific mRNA for degradation through an RNase mechanism or by sterically blocking the translation of the mRNA into the corresponding protein (Dias & Stein, 2002). They have been used in mouse models to study the specific function of genes and their corresponding protein products (Kola & Sumarsono, 1995; Pal, Zinkel, Kiessling, & Cooper, 1991; Richards, Carroll, Kinloch, Wassarman, & Strickland, 1993; Z. Tong, Nelson, & Dean, 1995). However, the application of antisense oligonucleotides is effectively limited by several difficulties, such as the potential displacement of the antisense oligonucleotides by ribosomal translational machinery, target inaccessibility (Dias & Stein, 2002), and limited efficacy due to the ability of the cell to replace lost mRNA (Mahato, Cheng, & Guntaka, 2005).

Alternatively, RNAi is an advanced sequence-specific post-transcriptional regulator of mRNA. These small RNA oligonucleotides are targeted to mRNA transcripts to induce either translation suppression or, more commonly, degradation of the mRNA (Mahato et al., 2005) The RNAi mechanism is a multistep process initiated when a precursor double-stranded RNA is processed by the RNase enzyme Dicer to generate small interfering RNA (siRNA) or micro-RNA (miRNAs), which become incorporated into the RNA-induced silencing complex (RISC).

The complex recognizes target mRNAs homologous to the siRNA or miRNA and translationally blocks or degrades them (Barton & Medzhitov, 2002; Mahato et al., 2005). In contrast to standard recombination assays, RNAi-based genetic

manipulation is a cheaper, relatively simple tool with the potential to efficiently produce desired phenotypes (Sarnova et al., 2010). RNAi strategies have been used in several studies and have provided significant progress in elucidating the molecular basis of key processes in oocytes (Arnold, Françon, Zhang, Martin, & Clarke, 2008; Fedoriw, Stein, Svoboda, Schultz, & Bartolomei, 2004; Han, Chen, Paronetto, & Conti, 2005; Igarashi, Knott, Schultz, & Williams, 2007). However, there are several potential problems with RNAi strategies, such as the labor-intensive process of obtaining effective RNAi molecules, effective delivery of RNAi molecules and non-robust phenotypic expression due to insufficient protein knockdown. Additionally, in cases in which transgenic RNAi is attempted, one potential problem is epigenetic silencing of the transgene, resulting in inconsistent expression of the transgene (Malik & Svoboda, 2012). These challenges suggest that alternatives to RNAi would be useful to study the functions of various genes in oocytes. Hence there is the need to develop fast, specific and cheap genetic manipulation strategies with the potential to generate more robust phenotypes.

Triplex forming oligonucleotides (TFOs) are sequence-specific single-stranded DNA molecules that interact specifically with homopurine sequences in the DNA duplex to form triple-stranded complexes called triplexes (Felsenfeld & Rich, 1957). Because of their sequence specificity and high binding affinity, TFOs can modulate transcription of the gene by blocking RNA polymerase (Kim et al., 1998; Postel, Flint, Kessler, & Hogan, 1991). This approach presents an opportunity to manipulate specific genes of interest prior to the occurrence of transcription. The limited number of each gene target (two alleles or copies of each) in contrast to the large number of

RNA targets potentially provides some advantage to use of TFOs over the antisense and RNAi approaches. Both RNAi and antisense strategies can block the translation of mRNA and target the mRNA for degradation but do not prevent further transcription of the corresponding gene to restore the mRNA pool. TFO-mediated inhibition of gene transcription can in theory significantly reduce the mRNA concentration, an effective approach with potentially long-term effects (Mahato et al., 2005). Hence the ability of TFOs to modulate gene expression could be used to drive new genome manipulation approaches in mammalian oocyte biology research.

## **2. Triplex-forming Oligonucleotides (TFOs)**

### **2.1 Chemistry of TFOs**

Initially discovered in 1957, triplex-forming oligonucleotides (TFOs) are single-stranded oligonucleotides that form a sequence specific triple helix by interacting with homopurine tracts in the major groove of the DNA duplex (Felsenfeld & Rich, 1957; Fox, 2000; Frank-Kamenetskii & Mirkin, 1995; Knauert & Glazer, 2001a; Radhakrishnan & Patel, 1994). Two sequence-specific binding motifs of triplex helix formation have been identified: the polypyrimidine and the polypurine motifs (Figure 1). As shown in Figure 1B, in the polypyrimidine motif TFOs, T recognizes A-T base pairs and protonated C recognizes G-C base pairs to form T.A-T and C.G-C base triads respectively by interacting through Hoogsteen hydrogen bonding in a parallel orientation to the purine strand of the duplex. In the polypurine motif, G recognizes G-C base pairs and A recognizes A-T bases pairs, interacting

through reverse Hoogsteen base pairing in an antiparallel orientation to the purine strand of the DNA duplex to form G.G-C and A.A-T base triads respectively (Figure 1C) (Chan & Glazer, 1997; Cooney, Czernuszewicz, Postel, Flint, & Hogan, 1988; Maher, Wold, & Dervan, 1989; Young, Krawczyk, Matteucci, & Toole, 1991). The stabilities of polypyrimidine triplexes are dependent upon pH because the N3 of the cytosines of the TFO must be protonated to provide the second Hoogsteen hydrogen bond to the N7 of the guanine in the target DNA duplex. The stability of purine motif triplexes are not pH dependent, though they can form G-rich intermolecular structures (Chan & Glazer, 1997; Escudéé et al., 1993; Radhakrishnan & Patel, 1994).

## **2.2 TFO modifications that Enhance Triplex Stability**

The interactions between deoxyribose polypyrimidine TFOs and their target DNA duplex are generally weak, forming triplexes of low thermal stability. However, for biological applications, triplexes are required to have strong binding affinity under physiological conditions to effectively modulate the expression of the targeted gene. Evidence suggests that modifications to the nucleotides of polypyrimidine TFOs can significantly improve the stability of triplexes (Campbell & Miller, 2009a; Campbell & Miller, 2009b; Graham & Miller, 2012). These include modifications of the cytosine bases, the sugars and/or phosphate groups of the sugar-phosphate backbone, and conjugation of the TFOs with an alkylating agent.

The requirement for protonation of the cytosines in deoxyribose polypyrimidine TFOs limits their application in cells because the intracellular pH is approximately 7.5. To circumvent this problem, deoxycytidines in polypyrimidine

TFOs can be replaced with 5-methylcytosines (Povsic & Dervan, 1989; Singleton & Dervan, 1992; Xodo, Manzini, Quadrioglio, van der Marel, & van Boom, 1991) or N<sup>6</sup>-methyl-8-oxo-2-deoxyadenosine (Krawczyk et al., 1992) to decrease the pH dependence and enhance the triplex formation and stability at higher pH.

It is possible to confer additional stability to the triplexes formed by polypyrimidine TFOs by replacing the deoxyribose sugar with 2'-O-methylribose (2'-OMe) (Faria et al., 2000). This modification increases the T<sub>m</sub> of the triplex compared to that of triplexes formed by polypyrimidine TFOs containing deoxyribose (Crooke, 1992; Graham & Miller, 2012) and increases the resistance of the TFO to nuclease degradation (Inoue et al., 1987).

The phosphodiester backbone can be modified to increase the triplex affinity and stability. These chemical modifications include phosphoramidates (Escudé, Sun, Rougée, Garestier, & Hélène, 1992), morpholino phosphoramidate linkages (Basye, Trent, Gao, & Ebbinghaus, 2001) and phosphorothioate linkages (Lacoste, François, & Hélène, 1997). The ability of the TFO to modulate the expression of the targeted gene depends on the duration of their interaction with the DNA duplex. The longer they interact with the target DNA duplex, the longer the antigene effect. Generally, unmodified TFOs have limited interactions with the target. The limited interaction of unmodified TFOs with their targets was first established by Young et al (1991), whose research demonstrated that unmodified TFOs can temporarily stall RNA polymerase and arrest transcription. However, RNA polymerase eventually displaces the TFO from the targeted DNA, resumes elongation and produces full-length transcript. However TFOs conjugated to a functional group that can covalently cross-link the

TFO to the target DNA, can effectively block transcription (Young et al., 1991). Consequently a variety of groups such as photoactivable psoralen (Besch et al., 2004; Giovannangeli, Thuong, & Hélène, 1992; Guieysse, Praseuth, Giovannangeli, Asseline, & Hélène, 2000; Havre, Gunther, Gasparro, & Glazer, 1993; Takasugi et al., 1991), platinum derivatives (Colombier, Lippert, & Leng, 1996) and bromoacetamide (Taylor & Dervan, 1997) have been studied for their ability to cross-link TFOs to their target DNA duplexes.

Platinum-derivatized TFOs (Pt-TFOs) have been studied for their ability to cross-link the TFO to the target duplex. Terminal guanine residues in the TFO can be reacted with transplatin to form a platinum derivatized TFO that, upon formation of the triplex, can react with the N7 of adjacent guanines in the target DNA duplex (Colombier, Lippert, & Leng, 1996). As shown in Figure 2A, the platinum residue is positioned at the N7 of the 3' terminal guanine of the TFO. Figure 2B shows the general structure of the platinated guanine and the coordination adduct formed by reaction of the platinum with a guanine. This allows the platinated guanine to reach across the major groove of the DNA duplex to form a cross-link with the adjacent G residue in the DNA duplex. This cross-link irreversibly links the TFO to the target duplex. When combined with nucleotide modifications, cross-link formation significantly enhances the stability of the triplex (Graham & Miller, 2012).

### 2.3 Biological Activities of TFOs

Several *in vitro* and *in vivo* studies have provided insights into the potential applications of TFOs. These include gene transcription inhibition and modifications to the gene structure through recombination and mutations (Faruqi, Seidman, Segal, Carroll, & Glazer, 1996; Faruqi, Datta, Carroll, Seidman, & Glazer, 2000).

Several reports have demonstrated the ability of TFOs to regulate gene expression through transcriptional inhibition. To inhibit transcription, TFOs can be targeted to the coding regions of genes (Cooney et al., 1988; Radhakrishnan & Patel, 1994), or to the promoter regions (Duval-Valentin, Thuong, & Helene, 1992; Maher et al., 1989; Young et al., 1991). TFOs targeted to the promoter regions have been shown to inhibit transcription *in vitro*, as well as *in vivo*, through studies with cultured cells (Kim et al., 1998; Postel, Flint, Kessler, & Hogan, 1991). For example, a TFO targeted to a region of the human *c-myc* promoter blocked the transcription of the promoter region *in vitro* (Cooney et al., 1988), inhibiting the expression of the *c-MYC* gene. Duval-Valentine et al (1992) also demonstrated that a 13-mer TFO targeted to the *E. coli B-lactamase* gene downstream of the *bla* promoter prevents transcription initiation by *E. coli* RNA polymerase (Duval-Valentin, Thuong, & Helene, 1992). In another experiment, using a phosphorothioate-modified polypurine TFO, and a luciferase reporter plasmid assay, Kim et al (1998) showed that a TFO targeted to the *c-myc* pro-oncogene in HeLa cells inhibited the transcription of the *c-myc* promoter as indicated by the decreased luciferase expression (Kim et al., 1998).

TFOs have the potential to induce structural modifications of a targeted gene through recombination and mutation. TFOs targeted to specific regions of genes in



mammalian cells can induce recombination presumably through recognition of the triplex as damage by the repair machinery of the cell. Faruqi et al (1996) observed that a psoralen-conjugated polypurine TFO targeted to a region between two supF mutants in a dual supF tRNA reporter simian virus vector induced homologous recombination in the vector when transfected into COS cells (Faruqi et al., 1996; Faruqi et al., 2000). Additionally, conjugation of TFOs to mutagens can induce site-specific mutagenesis (Faruqi et al., 2000; Vasquez, Narayanan, & Glazer, 2000; Wang, Levy, Seidman, & Glazer, 1995; Wang, Seidman, & Glazer, 1996).

### **3. Overview of Thesis Research**

The overall goal of this thesis project was to investigate the possibility of using platinated triplex-forming oligonucleotides (Pt-TFOs) to inhibit the expression of candidate genes that are important for meiotic maturation or fertilization of mouse oocytes. To accomplish this goal, Pt-TFO binding sites were first identified in three specific target genes (addressed below in Section 3.1). The interactions of selected Pt-TFOs with short DNA duplexes that contain the TFO binding site were then characterized. The uptake of fluorescein-derivatized TFOs by mouse NIH3T3 cells in culture was then investigated using fluorescence microscopy. Finally, the ability of a Pt-TFO to inhibit gene expression in mouse NIH3T3 cells was examined using RT-qPCR and western blot techniques.

### 3.1 Oocyte Target Genes

The target genes for these studies, *Cd9*, *Plk1* and *Cdc25b*, all contain homopurine tracts that are potential binding sites for Pt-TFOs.

#### 3.1.a *Cd9*

*Cd9* is a member of the Tetraspanins family of membrane proteins, which have unique structural features consisting of four transmembrane domains and extracellular amino and carboxy tail cytoplasmic subunits (See Figure 3B) (Glazar & Evans, 2009; Levy & Shoham, 2005). More than 30 tetraspanin homologues have been identified in mammals, and although they share evolutionally conserved structural features, they have distinct functions including regulation of cell motility, adhesion proliferation, differentiation, signaling and cell fusion (Boucheix & Rubinstein, 2001; Hemler, 2001). Tetraspanins appear to act as molecular facilitators, organizing membrane proteins such as integrins, tetraspanins, immunoglobulin superfamily members, and growth factor receptors to form stable macromolecular protein complexes in the plane of the membrane; these complexes are also known as tetraspanin webs (Berditchevski & Odintsova, 1999; Boucheix & Rubinstein, 2001; Hemler, 2003; Woods & Couchman, 2000). CD9 has a number of cellular functions, including regulating cell motility, cell adhesion, mitotic functions, signaling, membrane fusion, and proliferation (Le Naour, Rubinstein, Jasmin, Prenant, & Boucheix, 2000; Miller, Georges-Labouesse, Primakoff, & Myles, 2000).

As shown in Figure 3A, mouse CD9 consists of 8 exons spanning more than 23 kB (Le Naour et al., 2000). CD9 is expressed on the mouse egg plasma membrane (Chen & Sampson, 1999; Kaji, Oda, Miyazaki, & Kudo, 2002). Recent studies suggest

that CD9 is important for the interaction of egg and sperm membranes, a crucial step for fertilization. Knockout studies in mice showed that *Cd9*<sup>-/-</sup> female mice are infertile, though sperm could bind to the plasma membrane of zona pellucida-free oocytes isolated from the infertile female mice (Figure 3B) (Kaji et al., 2000; Le Naour et al., 2000; Miyado et al., 2000). When an individual sperm was injected into oocytes isolated from *Cd9*-deficient mice, fertilization was rescued and these injected oocytes produced zygotes that developed normally (Miyado et al., 2000). Alternatively, the ability of *Cd9*-deficient oocytes to be fertilized was restored when human *Cd9* mRNA or mouse *Cd9* mRNA was injected into the *Cd9*<sup>-/-</sup> oocytes (Le Naour et al., 2000; Zhu et al., 2002).

Additionally, *in vitro* fertilization experiments have also been used to study the effect of CD9 on egg-sperm interactions. In these experiments, zona-free eggs isolated from female mice were incubated in the presence of anti-CD9 mouse antibodies and inseminated with sperms, and co-incubated. Binding and fusion were assessed by microscopy (Chen & Sampson, 1999; Le Naour et al., 2000; Miller et al., 2000). Results from these studies demonstrated that oocytes treated with anti-CD9 mouse antibody had reduced sperm-oocyte fusion (Chen & Sampson, 1999; Le Naour et al., 2000; Miller et al., 2000). These results have been replicated in other models, including pigs (Li et al., 2004).

The combination of the anti-CD9 antibody and *Cd9* knockout mice studies suggests that CD9 is involved in sperm-egg gamete membrane interactions. The specific molecular role of CD9 in the molecular mechanism of this event(s) of fertilization is unknown. The sequence-specific interactions of Pt-TFOs can be

exploited as a genetic modulation technique to manipulate the expression of CD9 in oocytes, producing a new way to contribute to studies of the molecular interactions or functions of CD9 in oocyte research.

### **3.1.b Polo-like Kinase 1 (*Plk1*)**

Polo-like kinase 1 (PLK1) belongs to the family of conserved serine/threonine Polo-Like Kinases (PLK) that regulate the cell cycle and various mitotic stages including entry and exit into the M-phase, and spindle assembly (Glover, Hagan, & Tavares, 1998; Pahlavan et al., 2000; Strebhardt & Ullrich, 2006). Structurally, PLKs have a kinase domain at the amino terminus and a polo-box-binding domain at the carboxy terminus (Strebhardt & Ullrich, 2006). There are four mammalian PLK homologues, PLK1, PLK2, PLK3, and PLK4 (Glover et al., 1998; Pahlavan et al., 2000; Strebhardt & Ullrich, 2006).

PLK1 is a G2/M transition regulator with key roles in multiple processes such as cell proliferation, cell cycle progression, microtubule organization, and cytokinesis (Glover et al., 1998; Tong et al., 2002; Watanabe et al., 2004). Over-expression of *Plk1* has been associated with several malignancies such as non-small cell lung cancer, breast cancer, endometrium and ovarian cancer (Eckerdt, Yuan, & Strebhardt, 2005; Shi et al., 2010; Strebhardt & Ullrich, 2006; Takai, Hamanaka, Yoshimatsu, & Miyakawa, 2005). The *Plk1* homozygous null mutations in mice are embryonically lethal and *Plk1*<sup>-/-</sup> embryos do not survive (Lu et al., 2008), making it impossible to study fertilization. However, PLK1 was successfully targeted by a systemic (Dassie et al., 2009) and cell type-specific (McNamara et al., 2006) aptamer-siRNA combination

in prostate cancer cells expressing prostate-specific membrane antigen in mouse models. Based on this, we considered PLK1 as a potential target for TFO based gene inhibition studies.

Recent studies have highlighted the role of PLK1 in oocyte maturation and fertilization. Using immunocytochemistry studies and embryos isolated from matings of *Plk1*<sup>+/-</sup> mice, Lu *et al* 2008, demonstrated that *Plk1*-null embryos did not survive, past the early cleavage stages of development, suggesting that PLK1 may play a significant role in normal cell cycle progression (Lu et al., 2008). Using a combination of microinjection and immunoprecipitation studies, Ito *et al.*, 2008 demonstrated that overexpression of the PLK1 polo-box domain (*Plk1* PBD) mRNA in oocytes resulted in delayed Germinal Vesicle Breakdown (GVBD) during *in vitro* meiotic maturation, but the oocytes were still able to complete the GVBD stage, while an overexpression of a constitutively active *Plk1* substrate, CA (T210D)-*Plk1* mRNA, accelerated progression through meiotic maturation (Ito et al., 2008). Collectively, their research suggests that *Plk1* is required for maturation of oocytes. Furthermore, microinjection of anti-PLK1 mouse antibodies into mouse oocyte causes delayed germinal vesicle breakdown rate and distorted spindle organization during meiosis (Tong et al., 2002). As it is difficult to generate a viable knockout *Plk1* mouse, the sequence specificity of TFOs can potentially be harnessed to target the *Plk1* gene to inhibit its transcription to generate *Plk1*-deficient oocytes for studies.

### 3.1.c Cell division cycle 25b (*Cdc25b*)

Cell division cycle 25b (CDC25b) is a member of the cyclin division cycle 25 (CDC25) serine / threonine protein phosphatases that regulate cell cycle division by controlling the G2/M phase transition (Galaktionov & Beach, 1991). Structural features of the CDC25 phosphatases include the highly conserved C-terminal catalytic domain and the variable amino terminal regions. In mammals, there are three CDC25 homologues, CDC25a, CDC25b and CDC25c (Lindqvist et al., 2004; Sohn et al., 2004). CDC25B activates the CDK1-cyclin B complexes during G2/M and is involved in fundamental cell cycle control, thus affecting many cellular processes including cell growth, survival, and proliferation (Draetta & Eckstein, 1997; Galaktionov & Beach, 1991; Lindqvist et al., 2004).

In mammalian species, oocytes are arrested at prophase of meiosis I prior to ovulation (Sen & Caiazza, 2013). One of the most important mechanisms for resumption of meiosis and exit from this prophase I arrest is the activation of cyclin-dependent kinase-1 (CDK1) (Lincoln et al., 2002). Using *Cdc25b*<sup>-/-</sup> female mice, Lincoln *et al.* (2002) demonstrated that *Cdc25b* is required for meiotic resumption. Female mice deficient in *Cdc25b* were sterile, though their ovaries were normal (Lincoln et al., 2002). Microinjection of wild-type *Cdc25b* mRNA into oocytes from *Cdc25b*<sup>-/-</sup> females resulted in the resumption of meiosis (Lincoln et al., 2002). In rat oocytes, antibodies against CDC25b interfered with the oocyte's ability to undergo germinal vesicle breakdown (Gershon, Galiani, & Dekel, 2006).

In summary, the importance of the *Cd9*, *Plk1* and *Cdc25b* in fertilization and oocyte maturation has been demonstrated by a variety of studies, including analyses of

oocytes from knockout mice (in cases where these knockout animals are available and viable), and various methods to perturb function or expression of the proteins. However, these knockout methods are time-consuming, labor-intensive and costly. Targeting these genes with Pt-TFOs presents an opportunity to harness the sequence specificity and potential long-term effects of Pt-TFOs as a potential technique for modulating gene expression. Furthermore, with the advent of advanced and robust whole genome sequencing, the DNA sequences of genes involved in oocyte biology will be readily available and the successful initial applications of Pt-TFOs will set a precedent for new and effective direct gene modulation approaches for exploring the functions of key genes in oocytes.

### **3.2 Research approaches**

In the thesis research I used two experimental approaches, *in vitro* biochemical assays to characterize the biochemical properties of Pt-TFOs the triplex and *in vivo* biological assays using cultured mouse NIH3T3 cells. Pt-TFOs were designed based on identifying TFOs binding sites in the target genes using a web-based search engine. The *in vitro* experiments included characterizing the interaction of TFOs and Pt-TFOs with short DNA duplexes that contain the TFO binding sites using gel electrophoretic mobility shift assays and UV thermal denaturation experiments. The *in vivo* assays consisted of examining the uptake of fluorescein-derivatized inert Pt-TFOs (Inert Pt-TFO is chemically inactive and does not crosslink to the DNA target) by cultured mouse NIH3T3 cells with fluorescence microscopy and assessing the ability of the fluorescein-derivatized active Pt-TFOs to inhibit gene expression in mouse NIH3T3

cells using RT-qPCR and western blot techniques. The experiments performed are outlined below.

### **3.2. a Identification of Pt-TFO Binding Sites**

A web-based search engine (Gaddis et al., 2006) was used to identify homopurine tracts in mouse *Cd9*, *Plk1* and *Cdc25b* genes that could be targeted by Pt-TFOs. This search engine allows the user to search different regions of the genes including introns, exons, and promoters with specific parameters such as length of sequence, % GC, pyrimidine interruptions and options to mask repeated sequences (Gaddis et al., 2006). Homopurine tracts appear to be a surprisingly common feature of mammalian genes. For example, Wu et al. (2007) used the search engine to identify triplex-forming target sequences in the complete human and mouse genome and found at least one potential TFO binding site localized in the promoter and or transcribed regions in 97.8% of human and 95.2% of mouse genes (Wu et al., 2007). An additional consideration for finding Pt-TFO binding sites was the presence of a guanine residue adjacent to the TFO binding site that would enable the Pt-TFO to cross-link to the DNA target. As I will address below in Section 3.2.d, studies in this thesis research largely focused on *Cd9*-targeting TFOs.

### **3.2.b Interaction of TFOs and Pt-TFOs with their target binding sites**

The interactions of TFOs and Pt-TFOs containing either pyrimidine deoxyribo- or pyrimidine 2'-O-methylribonucleotides with short DNA duplexes were assessed by ultraviolet (UV) thermal denaturation experiments or by gel electrophoretic mobility



shift assays (EMSA) (Campbell & Miller, 2009a; Campbell & Miller, 2009b; Guieysse, Praseuth, Giovannangeli, Asseline, & Hélène, 2000; Havre, Gunther, Gasparro, & Glazer, 1993). Thermal denaturation experiments were used to assess the ability of TFOs to form triplexes with DNA duplexes containing their cognate binding sites. The thermal stability of the triplexes was monitored as a function of pH.

EMSA was used to determine the cross-linking efficiency of Pt-TFOs with their DNA targets. In these experiments the target DNA duplex is end labeled with a 5-terminal-<sup>32</sup>P-phosphate group. The labeled duplex is incubated with the Pt-TFO; the reaction mixture is subjected to electrophoresis on a denaturing polyacrylamide gel (PAGE); and the products of the reaction are detected by phosphorimaging the gel (Campbell & Miller, 2009a; Campbell & Miller, 2009b; Graham & Miller, 2012). The electrophoretic mobility of the labeled strand of the duplex that has cross-linked to the Pt-TFO is less than that of the non-cross-linked labeled strand of the duplex. Quantification of each labeled strand on the gel allows determination of the percent cross-linking by the Pt-TFO.

### **3.2.c Uptake of Fluorescein-Derivatized TFOs by Mouse NIH3T3 Cells in Culture**

As noted above, *in vivo* experiments consisted of examining the uptake of fluorescein-derivatized inert platinated TFOs (Inert Pt-TFOs) by cultured mouse NIH3T3 cells. This necessitated use of transfection as a non-viral based approach of transferring nucleic acids into mammalian cells (Malone, Felgner, & Verma, 1989; Noguchi, Furuno, Kawaura, & Nakanishi, 1998). There are a variety of transfection

methods including physical approaches such as microinjection and electroporation, and approaches that use transfection agents such as cationic liposome and polymers. While several transfection methods are available for cellular delivery of nucleic acids, they all have limitations in terms of transfection efficiency, cellular toxicity, and reproducibility.

One of the most significant challenges to nucleic acid transfection is traversing the plasma membrane with a hydrophilic, negatively charged nucleic acid. To circumvent this problem, commercially available cationic liposomal and polymers have been developed. Most cationic transfection reagents rely on the electrostatic interactions between the negatively charged nucleic acid phosphates and the positively charged head groups of the cationic lipid. These interactions effectively mask the negative charge of the nucleic acid, and impart an overall positive charge to the complex (Duan, Zhang, Wang, Yang, & Zhi, 2009). The mechanism(s) by which the DNA-cationic liposome/polymer complex enters the cell is not well understood, although studies suggest that the DNA-cationic liposome/polymer complex is taken up by endocytosis (Wrobel & Collins, 1995; Zabner, Fasbender, Moninger, Poellinger, & Welsh, 1995). Once in the cell, the complex dissociates the endosome and releases the nucleic acid into the cytoplasm where it is subsequently distributed to different cellular compartments (Crooke, 1992; Felgner et al., 1987; Felgner & Ringold, 1989; Noguchi et al., 1998).

The ultimate destination of the nucleic acid could be affected by the composition of the transfection agent. Therefore we performed comparative in vivo studies of two commercially available transfection agents, liposomal cationic

Lipofectamine™ 2000 and the cationic polymer FuGENE HD. Both transfection agents were assessed for their cellular delivery, uptake efficiency and nuclear localization of a fluorescein labeled inert Pt-TFO in NIH3T3 mouse fibroblast cells. The number of cells with fluorescein-labeled inert Pt-TFO compared to the number of endogenous DNA per image was used to estimate the uptake efficiency. Three independent fields of cells were analyzed and the results averaged.

### **3.2.d Biological Effects of a *Cd9*-Targeting Pt-TFO Mouse NIH3T3 Cells in Culture**

The ability of a Pt-TFO to inhibit *Cd9* gene expression was evaluated using (1) a standard reverse transcriptase quantitative polymerase chain reaction (RT-qPCR) to assess changes in mRNA transcript levels; and (2) western blotting to evaluate any reduction in CD9 protein expression. In both assays, cells treated with either a scrambled Pt-TFO and a *Cd9*-specific TFO were compared to control cells treated with only transfection agent.

Given the results of preliminary screening experiments, which indicated that the deoxy-*Cd9* specific TFOs had significant binding affinity to the *Cd9* DNA target and the platinated *Cd9*-specific TFOs effectively cross-linked to their target DNA, we selected the *Cd9* target gene for further studies. Hence, the bulk of the thesis research focuses on the *in vitro* characterization and *in vivo* investigation of the inhibitory effects of *Cd9*-specific TFOs.

## **MATERIALS AND METHODS**

All reagents were purchased from Sigma (St. Louis, MO) unless otherwise noted. Sso Advanced SYBR Green was purchased from (Bio-Rad, CA). Monoclonal rat anti-mouse antibody to CD9 (BD Biosciences, CA) and HRP-conjugated goat anti-rat IgG (80 ng/ml) were obtained from Janice Evans' Lab (BMB, JHSPH). Monoclonal anti-beta-actin antibody (0.5 mg/ml stock) and HRP-conjugated goat anti-mouse IgG (0.5 mg/ml) were generously provided by Pierre Couloumbe's Lab (BMB, JHSPH). 2'-0 -methoxyribo-5-methylcytosine and 2'-0 -methoxyribothymine phosphoramidites were purchased from ChemGenes (Ashland, MA) and 6-fluorescein phosphoramidites were purchased from Glen Research (Sterling, VA). NIH3T3 mouse fibroblast cells (generously provided by Pierre Coloumbe's Lab -JHSPH BMB).

### **1. Cell culture and TFOs and transfections**

NIH3T3 mouse fibroblast cells were maintained in Dulbecco's Modified Eagle Medium (DMEM) (Gibco/Invitrogen, Carlsbad, CA) supplemented with 10% fetal bovine serum (Gibco/Invitrogen, Carlsbad, CA), 100 U/mL penicillin, and 100 µg/mL streptomycin incubated at 37°C with 5% CO<sub>2</sub>.

### **2. Oligonucleotides design**

The sequences of all TFOs (except Scrambled TFO) were obtained using the Triplex-Forming Oligonucleotide (TFO) Target Sequence Search (Gaddis et al., 2006) using the following criteria: Species-mouse, minimum TFO target sequence length of 15

nucleotides, a minimum 50% Guanine content, with or without pyrimidine interruptions.

The extinction coefficients of all TFOs were calculated using the Oligo Calc:

Oligonucleotide Properties Calculator (Kibbe, 2007). The sequences of all

oligonucleotide and the DNA duplexes used are given in Table 1.

### **3. Oligo-2'-O-methylribonucleotides synthesis**

The 2'-O-methylribonucleotide-modified oligonucleotides containing 2'-O-methoxyribo-5-methylcytosine, 2'-O-methoxyribothymine, 6-carboxyfluorescein (6-FAM) conjugated to the 5' end of the TFO) and deoxyriboguanosine were synthesized on an Applied Biosystem ABI 3400 automated DNA/RNA synthesizer. All phosphoramidites used in the synthesis were prepared as 0.15 M solutions and the oligonucleotides were synthesized on a controlled pore glass (CPG) containing 1  $\mu\text{mol}$  of the terminal 3' nucleotide of each sequence. The coupling reactions were activated by 5 ethylthiotetrazole, and coupled at 360 s for all 2'-O-methylribonucleotide phosphoramidites and 120 s for deoxyribonucleotides. Following synthesis, the CPG-bound oligonucleotides were washed with 10 mL of dry acetonitrile, and dried on a vacuum pump. The CPG-bound oligonucleotides were dissolved in a solution of 300  $\mu\text{L}$  of concentrated ammonium hydroxide and 100  $\mu\text{L}$  of 95% ethanol and incubated at 55<sup>o</sup>C for 18 hours to deprotect and release the oligonucleotides from the CPG support. The supernatant was removed, and the supports were washed four times with 200  $\mu\text{L}$  of 50 % aqueous acetonitrile. The supernatants were combined and evaporated to dryness on a SpeedVac concentrator. The residue was redissolved in 500  $\mu\text{L}$  of 50% acetonitrile and stored at 4<sup>o</sup>C. The purities of the oligonucleotides were confirmed by strong anion

exchange high-performance liquid chromatography (HPLC) on a Dionex DNAPac PA 100 4 mm x 250 mm column (Dionex, Sunnyvale, CA, USA) using 0-0.5 M sodium chloride in a buffer containing 100 mM tris (hydroxymethyl) aminomethane (pH 7.8) and 10% HPLC grade methanol at a flow rate of 1.0 mL/min over a 30 min gradient. To confirm the compositions of the TFOs, matrix matrix-assisted laser desorption/ionization time-of-flight (MALDI-TOF) was performed at the Johns Hopkins School of Medicine AB Mass Spectrometry/Proteomics Facility.

Fluorescein-labeled 2'-0-methylribonucleotides oligonucleotides were synthesized as described above with the addition of 6-fluorescein phosphoramidites.

#### **4. Platination of TFOs**

Eleven nmol of TFO were evaporated to dryness on a SpeedVac and the residue, redissolved in a buffer containing 400  $\mu$ L of water and 100  $\mu$ L of 1 mM trans - diamminedichloroplatinum(II) dinitrate, and the solution incubated for 1 h at 37<sup>0</sup>C. The platinated TFO was purified by HPLC and desalted on a Waters Sep-Pak-Vac column (Waters, Milford, MA). The UV absorption spectra of the Pt-TFOs were recorded and their concentrations determined using extinction coefficients determined from an oligonucleotide properties calculator (Kibbe, 2007).

#### **5. Thermal denaturation experiments**

Triplex formation and stability were determined by recording a UV melting curves. For each reaction, a solution of 0.5  $\mu$ M of DNA duplex and 0.5  $\mu$ M of TFO or platinated TFO in 1mL of triplex buffer (pH 6.0, 7.0, or 7.5), containing 50 mM 2-(N - morpholino) ethanesulfonic acid, 100 mM NaCl, and 5 mM MgCl<sub>2</sub> was heated to 90<sup>0</sup>C

for 10 minutes in a sand bath and slowly cooled to room temperature. The absorbances of the triplex solutions were monitored in a Cary 3E UV-vis spectrophotometer as a function of temperature over the range 5°C to 85°C at a heating rate of 0.4°C/min. The normalized hyperchromism of the absorbance, calculated using the formula  $(A_1 - A_0) / (A_f - A_1)$  (where A indicates absorbance, 0-varying, 1-initial, f-final), was plotted against the temperature to determine the melting temperature of triplex.

## **6. Denaturing gel electrophoretic mobility shift assays (EMSA)/ cross-linking**

To study the interactions of the Pt-TFO with the DNA duplex, an electrophoretic mobility shift assay was carried out using  $^{32}\text{-P}$  as tracer. A 1  $\mu\text{M}$  solution of the purine-containing strand of the target duplex was labeled with a solution containing 1  $\mu\text{L}$  of T4 polynucleotide kinase, 10  $\mu\text{L}$  of ATP and  $\gamma$ - [ $^{32}\text{P}$ ]ATP (specific activity 10  $\mu\text{Ci}/\text{mmol}$ ), and 3.2  $\mu\text{L}$  of water. To remove unreacted  $^{32}\text{-P}$  ATP, the reaction was run through a G-25 spin column. An equimolar amount of the unlabeled complementary strand was added and the solution was evaporated to dryness on a Speed Vac. Triplex buffer (of varying pH, 250  $\mu\text{L}$ ) was added to the mixture, the solution was incubated at 60°C for 10 minutes, cooled to room temperature and stored at 4°C. To analyze cross-link formation, 10  $\mu\text{L}$  of the  $^{32}\text{-P}$  labeled duplex was added to increasing concentrations of the TFO (0-10  $\mu\text{M}$ ) and incubated at 37°C overnight. Ten microliters of gel loading buffer (80% formamide, 0.03% bromophenol blue, and 0.03% xylene cyanol) was added to each reaction mixture and a 10  $\mu\text{L}$  aliquot of the solution was subjected to electrophoresis at 800 V on a 20% denaturing polyacrylamide gel (18 cm x 20 cm) in tris (hydroxymethyl) aminomethane–borate–EDTA buffer. The gel was imaged on a FujiFLA-7000 phosphorimager and the

percent cross-linking was determined by comparing band densities using ImageGuage.

## **7. Transfection of NIH3T3 cells with TFO**

To investigate the effects of the TFOs on expression of the CD9 gene in NIH3T3 cells in culture, NIH3T3 cells grown to 80% confluency were seeded into 35mm cell culture dishes at  $8 \times 10^5$  cells per dish and incubated overnight. The cells, which were approximately 30-40% confluent, were then transfected with TFO. For all protocols, two transfection reagents FuGENE HD (Promega Madison, WI) and Lipofectamine TM 2000 (Carlsbad, CA) in a 1:3 DNA: transfection reagent ratio were used to determine the optimal transfection reagent.

For FuGENE HD transfections, 4  $\mu\text{g}$  of Pt-TFO (20  $\mu\text{L}$  of 200  $\text{ng}/\mu\text{L}$  fluorescein-labeled CD9 T2 3' TFO or fluorescein-labeled Scrambled 3' TFO) were diluted with 100  $\mu\text{L}$  of Opti-MEM (Invitrogen, Carlsbad, CA) and 12  $\mu\text{L}$  of FuGENE HD was diluted with 100  $\mu\text{L}$  of Opti-MEM. The two solutions were mixed by pipetting 15 times and incubated for 15 minutes. Complete growth medium was removed from the seeded NIH3T3 cells and replaced with 200  $\mu\text{L}$  of DNA : FuGENE HD complex and 1.8 mL of NIH3T3 complete growth medium. The reaction mixture was incubated for 72 hours without medium change and prepped or harvested for specific assays.

For Lipofectamine 2000 transfections, 2  $\mu\text{g}$  of Pt-TFO (10  $\mu\text{L}$  of 200  $\text{ng}/\mu\text{L}$  fluorescein-labeled CD9 T2 3' TFO or fluorescein-labeled scrambled 3' TFO) was diluted in 250  $\mu\text{L}$  of Opti-MEM. Lipofectamine 2000 (6  $\mu\text{L}$ ) was diluted in 250  $\mu\text{L}$  of Opti-MEM and the solution incubated for 15 minutes. The diluted DNA and diluted Lipofectamine 2000 were gently mixed by pipetting and incubated for 20 minutes.



Complete growth medium was removed from the seeded cells and replaced with 500  $\mu$ L of DNA: Lipofectamine 2000 complex in 1.5mL of Opti-MEM. The cells were incubated for 2 hours in the transfection medium, after which it was removed and replaced with regular cell culture medium. The transfection was repeated 24 hours after the initial transfection and the cells incubated for 48 hours post second transfection before prepping or harvesting for specific assays.

Negative control experiments were performed for all transfections where cells were either treated with just FuGENE HD or Lipofectamine 2000.

## **8. Cellular uptake and localization**

NIH3T3 cells were seeded on glass bottom wells and transfected with inert Pt-TFOs using FuGENE HD and Lipofectamine 2000 as previously described. 72 hours post transfection (FuGENE) or 48 hours post second dose transfection (Lipofectamine), the cells were fixed with a solution of 1 mL of phosphate-buffered saline [PBS] (Quality biological, Gaithersburg, MD) and 3.2  $\mu$ L of 1ng/ $\mu$ L Hoechst stain (Invitrogen) for 25 minutes. Live cell images were acquired using a Zeiss 510 Meta LSM microscope with Zeiss software. Three random images were captured and averaged for uptake efficiency, which was estimated by calculating the ratio of cells exhibiting green fluorescence from the inert Pt-TFO to those exhibiting blue fluorescence from the Hoechst staining of DNA. 40X images were captured to determine where the TFO were localized in the transfected cells.

## **9. RT-qPCR**

NIH3T3 cells were transfected with fluorescein-labeled scrambled and CD9 3'

Pt TFOs using FuGENE HD and Lipofectamine 2000 following the previously describe protocol, although the number of cells seeded and amount of all reagents used were doubled. That is  $16 \times 10^5$  cells were transfected, 8  $\mu\text{g}$  of Pt-TFO (40  $\mu\text{L}$  of 200  $\text{ng}/\mu\text{L}$ ) and 24  $\mu\text{L}$  of FuGENE HD were used for FuGENE HD transfection and 4  $\mu\text{g}$  of Pt-TFO (20  $\mu\text{L}$  of 200  $\text{ng}/\mu\text{L}$  of Pt-TFO) and 12  $\mu\text{L}$  of Lipofectamine 2000 were used for each Lipofectamine 2000 transfection (transfection repeated 24 hours after the first transfection). Seventy-two hours post transfection (FuGENE) or 48 hours post second transfection (Lipofectamine), the cells were trypsinized for 5 minutes at  $37^\circ\text{C}$ , centrifuged at 300  $\times\text{g}$  for 5 minutes and the supernatant discarded. The cells were washed again with 2 mL PBS and centrifuged at 300  $\times\text{g}$  for 5 minutes and the supernatant discarded. Total RNA was extracted from the cells using an RNase Mini Kit (Qiagen, Valencia, CA, Cat#74106) according to the manufacturer's instructions. Primers for CD9 were adapted from Huang et al. (2011) and primers for GAPDH (PrimerBank ID 6679937a1) were designed using the PrimerBank search engine (Harvard/MGI). CD9 primers were F- 5' -CTGGCATTGCAGTGCTTGCTA-3', R- 5' -AACCCGAAGAACAATCCCAGC-3' and GAPDH primers were F- 5' -AGGTCGGTGTGAACGGATTTG-3' and R-5' -TGTAGACCATGTAGTTGAGGTCA-3' (Huang et al, 2011). For real time reverse transcription quantitative polymerase chain reaction (RT-qPCR), 1  $\mu\text{g}$  of RNA was reversed transcribed using a solution of 1  $\mu\text{L}$  of SYBR green master mix and 4  $\mu\text{L}$  of 5x reaction mixture and excess nuclease free water at a final volume of 20  $\mu\text{L}$ . The cDNA reaction mixtures were diluted with 60  $\mu\text{L}$  of nuclease free water. The resulting cDNAs were stored frozen at  $-20^\circ\text{C}$  for further use. For each qPCR reaction, 8  $\mu\text{L}$  of the cDNA reaction mixture, 1.5  $\mu\text{L}$  of 5  $\mu\text{M}$  forward

and reverse primers, 10  $\mu$ L of SsoAdvanced SYBR Green supermix ( Bio-Rad, Hercules, CA ) and 0.5  $\mu$ L of nuclease-free water were mixed together. RT-qPCR was performed in a Bio-Rad 7000 thermocycler using the following thermocycle profile which was adapted from Weimin et al (2011): 5 minutes at 50°C, 10 minutes at 94°C, followed by 40 cycles of 15 seconds at 94°C and 1 minute at 60°C.

To optimize the conditions for the qPCR, a standard curve was prepared as follows:  $16 \times 10^5$  NIH3T3 cells were seeded in a 60mm cell culture plate and incubated for 72 hours and total RNA were extracted and reverse transcribed to cDNA as described above. Five, 1:10 serial dilutions of the cDNA were prepared qPCR was performed on each dilution following the Weimin's protocol as previously described. The Cycle threshold (Ct) values for each dilution were plotted against the log of the cDNA concentration resulting in a linear graph. Excel statistical functions were used to determine the slope and  $R^2$  value of the linear graph. PCR efficiency was calculated using the slope and efficiency calculator from Thermo Fisher Scientific (qPCR efficiency calculator).

## **10. Statistical Analysis**

For treated and untreated cells, the  $2^{-\Delta\Delta Ct}$  relative quantitative method was used to assess changes in the target genes expression post transfection.  $2^{-\Delta\Delta Ct}$  is used to quantify the amount of target genes in a treated sample that is normalized to an endogenous reference gene and compared to the expression of the target gene in a untreated control sample (Livak & Schmittgen, 2001). The  $2^{-\Delta\Delta Ct}$  was calculated as follows:

$$\Delta Ct (\text{treated cells}) = Ct (\text{CD9 target gene}) - Ct (\text{Gapdh reference gene})$$

$\Delta\text{Ct (untreated/negative control)} = \text{Ct (CD9 target gene)} - \text{Ct (Gapdh reference gene)}$

$\Delta\Delta\text{Ct} = (\Delta\text{Ct treated cells} - \Delta\text{Ct untreated})$

And fold change =  $2^{-\Delta\Delta\text{Ct}}$

All the results are shown as averages +/- standard deviation. All the data were analyzed using Microsoft Excel statistical functions.

## 11. Western Blots

NIH3T3 cells were transfected with fluorescein-labeled scrambled and CD9 3' Pt TFOs using FuGENE HD and Lipofectamine 2000 as previously described. Seventy-two hours post transfection (FuGENE HD) or 48 hours post second transfection (Lipofectamine 2000), the cells were washed in 2 mL ice cold phosphate-buffered saline [PBS] (Quality biological, Gaithersburg, MD) and 250 mL of cold Lysis buffer (50 mM of Tris-HCl, pH 7.6), 150 mM NaCl, 1% Triton-x-100, 0.5% Sodium Deoxycholate, and 4.68 mL ddH<sub>2</sub>O). 0.25  $\mu\text{L}$  of Protease inhibitor cocktail inhibitor (Sigma, St. Louis, MO) was added immediately. A cold plastic cell scraper was gently used to scrape the adherent cells for a few minutes and the cells were maintained at constant agitation for 30 minutes at 4°C. The cell suspension was then transferred to a pre-cooled centrifuge tube and centrifuged at 12000 X g at 4°C for 15 minutes. The supernatant was removed and placed in a fresh pre-cooled tube, and the pellet was discarded. The protein concentrations were measured using a Nanodrop spectrophotometer. The protein was stored frozen at 4°C until further use. Forty micrograms of untreated, fluorescein-labeled scrambled 3' Pt-TFO, fluorescein-labeled CD9 3'Pt-TFO protein samples were added to

10  $\mu$ L of 2X sodium dodecyl sulfate-polyacrylamide gel electrophoresis gel electrophoresis (SDS-PAGE) sample buffer and briefly centrifuged. As a positive control for CD9 on the immunoblot, 20 ng mouse liver lysate were prepared from a 5  $\mu$ g/ $\mu$ L stock solution of liver lysate. Fifteen  $\mu$ L of protein sample and 10  $\mu$ L of protein marker (Bio-Rad, Hercules, CA, Cat#161-0374) were loaded onto a non-reducing 12.5% SDS-PAGE and the gel was run for 1.5 h at 1500V. Resolved proteins on the gel were transferred to a piece of immobilon (Millipore, Billerica, MA) following a standard transfer protocol at 100 V for 1.30 hours. After the transfer, the blot was divided into two, and each membrane was blocked overnight in PBS containing 5% BSA and 0.1% Tween-20. The lower portion of the membrane was incubated in 1: 5000 dilution of KMC8.8, a rat monoclonal CD9 antibody (1mg/ml stock, BD Bioscience, San Jose, CA) in PBS with 0.1% Tween and 3% bovine serum albumin [BSA] overnight to probe for CD9 protein. The upper portion of the membrane was probed for beta-actin by incubating the membrane with a 1: 5000 dilution of monoclonal anti beta-actin mouse antibody in PBS containing 0.1% Tween and 3% BSA. The lower and upper portions of the membrane were washed four times in a solution containing PBS and 0.1% Tween for 15 minutes each and then incubated with 1:5000 HRP-conjugated goat anti-rat IgG (Janice Evans Lab) in a solution containing PBS, 0.1% Tween and 3% BSA for 1 hour and 1: 2000 HRP-conjugated goat anti-mouse IgG (Pierre Couloumbe Lab) in a solution containing PBS, 0.1% Tween and 3% BSA for 1 hour respectively. The blot was then washed 8 times in a solution containing PBS and 0.1% Tween for 2 hours and detected with a 1:1 dilution of ECL Supersignal West Pico Substrate (Pierce, Rockford, IL) for 5 minutes. Protein bands were visualized with FluorChem HD2 system and quantitative

analysis performed with ImageJ software (<http://rsbweb.nih.gov/ij/>).

## RESULTS

In the following experiments, two forms of platinated TFOs are used. TFOs are either platinated with an active N7-trans-diaminechloroplatinum- or inert N7-diethelentramineplatinum-deoxyguanosine residue. The active Pt-TFOs can cross-link to guanine residues in their target DNAs. This reaction anchors the TFO to the target DNA. The inactive Pt-TFOs are not chemically reactive and therefore unable to cross-link to their targets. Throughout the thesis Pt-TFO denotes a TFO with an active platinum and inert Pt-TFO denotes a TFO with an inactive platinum.

### **1. Selecting Pt-TFO Sequences to Target Homopurine Tracts in *Cd9*, *Plk1*, and *Cdc25b*.**

We used the triplex forming oligonucleotide search engine (Gaddis et al., 2006) to identify homopurine tracts in the *Plk1*, *Cd9* and *Cdc25b* genes that would be amendable to triple helix formation and cross-linking. Several potential target sequences were included in the results. To select specific TFO sequences for studies, we used criteria that have been defined through experimental studies of triplexes, based on factors that generally stabilize triplex formation. These factors serve as predictors of triplex stability and are used to select potential TFO sequences. They include the nucleotide length and composition of the TFO sequence, purine interruptions (Campbell & Miller, 2009a; Sandström, Wärmländer, Gräslund, & Leijon, 2002), low cytosine content, position of the terminal guanine and specific strand of the DNA duplex the TFO interacts with (Graham & Miller, 2012). Generally,

the stability of the TFO increases with increasing length. However, for our purposes, a minimum of length of 15 nucleotides with no more than one purine interruption was used to select the TFO sequences as purine interruptions tend to destabilize the triplex formation (Campbell & Miller, 2009a). Additionally, TFO sequences with contiguous cytosines residues were avoided due to the pH dependency of the C.GC triads. Furthermore, TFOs with terminal guanine on the 3' end of the TFO tend to form more stable triplexes than those with 5' terminal guanine and were preferred, though we selected sequences with either the terminal guanine on the 3' or 5' end and sometimes on both 3' and 5' ends to study the effects of the guanine on triplex stability. Finally, we selected TFOs that bind to and cross-link to the transcribed strand of the DNA because they have the potential to induce greater inhibition of gene expression. However, we made exceptions for these if the TFO conformed to the other parameters. These criteria should produce a TFO that can theoretically bind and cross-link to the target sequence. Therefore, the TFO sequences that conformed to the specified criteria were chosen for preliminary studies and are presented in Table 1. 3' TFO denotes TFOs with the terminal guanine on the 3' end of the TFO and the 5' TFO denotes TFOs with the terminal guanine on the 5' end.

## **2. Interactions of TFOs and Pt-TFOs with DNA Duplexes**

Two of the most commonly used methods to identify TFOs and Pt-TFOs that could bind efficiently to homopurine tracts in the gene targets are UV thermal denaturation and electrophoretic mobility shift assay (EMSA). In these assays the



experiments are performed using short DNA sequences corresponding to the target DNA duplexes.

The multistep process begins with performing thermal denaturation assays at three pH conditions (6, 7 and 7.5) to screen a panel of deoxyribose-TFOs to identify those with at least 35°C melting temperatures ( $T_m$ ) at physiological pH (7~7.5). We initially examined deoxyribo-TFOs because they are readily obtained from commercial sources and contain no base or backbone modifications.

In general, deoxy-TFOs form triplexes of low stability because the B-conformation of these TFOs is not compatible with the A-like conformation of the triplex. Although most deoxyribo-TFOs will form stable triplexes at low pH (pH 6); the binding results at pH 6 cannot be completely relied upon as predictors of triplex binding stability under physiological conditions. Because deoxyribo-TFOs rarely form stable triplexes at pH 7.5 or above (Graham & Miller, 2012), in our experiments  $T_m$  values were determined at pH 7. Based on the results of these binding experiments, deoxyribo-TFOs giving the most stable triplexes were selected, platinated with active transplatin and their ability to cross-link to target DNA assessed by EMSA.

Studies suggest that the 2'-O-methylribose TFO modification increases the  $T_m$  of the triplex by at least 30°C (Graham & Miller, 2012). Based on these observations, and the results from melting experiments with the deoxyribo-TFOs and cross-linking experiments with deoxyribo-Pt-TFO, deoxyribo-TFOs with high  $T_m$  that can cross-link to their DNA targets when platinated were selected for modification with 2'-O-methylribonucleotide residues. The  $T_m$  values of triplexes formed by these 2'-O-methylribo-TFOs were determined and those 2'-O-methylribo-TFOs that gave high  $T_m$

values under physiological conditions (pH 7.5) were selected, platinated with active transplatin and their abilities to cross-link to their targets were assessed using EMSA.

## 2.1 Deoxyribo-TFOs and Pt-TFOs

The thermal stabilities of triplexes formed by deoxyribo-TFOs with DNA duplexes containing the cognate binding site were examined using UV thermal denaturation experiments. Solutions containing equimolar concentrations of the deoxy-TFO and target DNA duplex in pH 7.0 triplex buffer were heated at 90°C for 10 min and then allowed to slowly cool to room temperature. The absorbance of the solution at 260 nm was monitored as the solution was heated at a rate of 0.4°C/min over a temperature range of 4-85°C. The normalized hyperchromicity  $(A_0 - A_1)/(A_f - A_1)$  (where A indicates absorbance, 0-varying, 1-initial, f-final), was plotted against temperature to determine the melting temperature of the triplex. Figure 4A shows a typical melting curve. The melting curve of the triplex (black curve) reveals two transitions: the first transition corresponds to melting of the third strand and the second transition corresponds to melting of the duplex into its respective single strands. The melting curve of the duplex alone (red curve) reveals one transition, which corresponds to the melting of the duplex into single strands.

Figure 4B shows the melting temperatures of the third strand of the triplexes formed by TFOs that target *Cd9*, *Plk1* and *Cdc25b* DNA at pH 7.0. All triplexes were stable at 20°C, though some bound with higher stability to their target than others. *Cd9* T1 3' TFO and *Cd9* T1 TFO 5' TFO had the highest  $T_{ms}$ , 42°C and 45°C respectively

(Fig. 4B). All the *Cd9* T2 TFO (18 nucleotides) had similar  $T_m$ s, with *Cd9* T2 3' TFO, *Cd9* T2 5' TFO, *Cd9* T2 3' and 5' TFO having melting temperatures of 38°C, 36°C, 38°C respectively (Fig. 4B). Similarly, *Cd9* T3 3' TFO, *Cd9* T3 5' TFO (19 nucleotides) had slightly higher melting temperatures of 40°C and 39°C. *Cd9* T6 5' TFO had a  $T_m$  of 34 °C and *Cdc25b*-T1 5' TFO had a  $T_m$  of 34 °C. However, *Plkl* T2 3' TFO, *Cdc25b*-T1 3' TFO, *Cdc25b*-T2 3' TFO and *Cdc25b* T2 5' TFO had the lowest melting temperatures, 27 °C, 23°C, 27°C and 27°C respectively (Fig. 4B).

The abilities of the platinum-derivatives of the TFOs described above to cross-link to their DNA targets were then examined. The 3'- or 5'-terminal guanines of the TFOs were platinated by reacting the TFO with trans- diaminediaaquaplatinum (II) dinitrate. The Pt-TFOs were purified by strong anion exchange (SAX) HPLC. The platinated TFO (0-100 pmol) was reacted with its target DNA duplex (10 pmol), whose purine strand was end labeled with  $^{32}\text{P}$  at 37°C. The reaction mixture was subjected to electrophoresis on a denaturing polyacrylamide gel. The gel was scanned by a phosphorimager and the percentage of cross-linking was determined from band intensities using Image Gauge software. The cross-linking reactions were performed in triplicate.

A representative gel is shown in Figure 5A, where the slower migrating band corresponds to the Pt-TFO cross-linked to the labeled purine strand of the duplex. The extent of cross-linking increased with increasing concentration of Pt-TFO. Figure 5B shows the percent cross-linking of 10  $\mu\text{M}$  deoxyribo-Pt-TFOs to their cognate DNA targets. At pH 6.0, all of the deoxyribo-Pt-TFOs cross-linked to their respective targets with varying efficiencies. Eight percent of *Plkl* 3' Pt-TFO cross-linked to its

duplex DNA, while only 2% of *Cdc25b* T1 3' Pt-TFO cross-linked to its target DNA (Fig. 5B). Sixty-one percent of *Cdc25b* T1 5' Pt-TFO cross-linked to its target, and 3% of *Cdc25b* T2 3' Pt-TFO cross-linked to its target and 45% of *Cdc25b* T2 5' Pt-TFO cross-linked to its target. The highest levels of cross-linking were observed for Pt-TFOs that targeted *Cd9* (Fig. 5B). Fifty-five percent of *Cd9* T1 3' Pt-TFO cross-linked to their targets, while 73% of *Cd9* T1 5' Pt-TFO cross-linked to their targets. Thirty-one percent of *Cd9* T2 3' Pt-TFO cross-linked to its target while 73% and 73 % of *Cd9* T1 3' Pt-TFO, *Cd9* T2 5' Pt-TFO cross-linked to their targets respectively. Nineteen percent of *Cd9* T3 3' Pt-TFO, 45% of *Cd9* T3 5' TFO and 12% of *Cd9* T6 5' Pt-TFO cross-linked to their targets (Fig. 5B).

The extent of cross-linking is dependent upon pH. At pH 7.0, neither *Plk1* 3' Pt-TFO, *Cdc25b* T1 3' Pt-TFO, *Cdc25b* T1 5' Pt-TFO, *Cdc25b* T2 3' Pt-TFO, *Cdc25b* T2 5' Pt-TFO cross-linked to their targets. Additionally, only 2% of *Cd9* T1 3' Pt-TFO and 3% of *Cd9* T1 5' Pt-TFO cross-linked to their targets. *Cd9* T2 3' Pt-TFO had the highest cross-linking efficiency, with 14% of the Pt-TFO cross-linking to its target, while only 6% of *Cd9* T2 5' Pt-TFO cross-linked to its target despite having similar melting temperature and similar nucleotide composition. Surprisingly, *Cd9* T2 3' and 5' Pt-TFO did not cross-linked to its target DNA. Twelve percent of *Cd9*T3 3' Pt-TFO cross-linked to its target and 11% of *Cd9* T3 5' Pt-TFO cross-linked to its target and only 4% of *Cd9* T6 5' Pt-TFO cross-linked to its target (Fig. 5B).

## 2.2 2'-O-Methylribo-TFOs and Pt-TFOs

Based on the binding and cross-linking results, the *Cd9* T2 3' TFO and *Cd9* T2 5' TFO sequences were chosen for further study. *Cd9* T2 3' TFO had the highest cross-linking (14%) despite having a  $T_m$  of 38°C and *Cd9* T2 5' TFO had a  $T_m$  of 36°C and a slightly lower cross-linking of 6%. Previous studies have shown that 2'-O-methylribo-Pt-TFOs have increased binding and cross-linking efficiency and are less susceptible to nuclease digestion in comparison to their deoxyribo-counterparts (Campbell & Miller, 2009a; Graham & Miller, 2012). To determine if similar results could be achieved with the *Cd9*-specific TFOs, we synthesized modified *Cd9* T2 3' and 5' TFO with a 2'-O-methylribonucleotide backbone, 5-methylcytosines, 5-methyluridine, and deoxyguanosines at the 3' or 5' ends using a standard automated synthesis procedure. HPLC analysis indicated the presence of two distinct peaks for both *Cd9* T2 3' and 5' TFO, which could indicate cleavage of the oligonucleotide or incomplete synthesis. Mass spectrometry was performed to determine which peak corresponded to the desired TFO. The expected mass for both 2'-OMe *Cd9* T2 3' TFO and 5' TFO is 5944.1 (Table 2). For both TFOs, samples from the second peak of the HPLC chromatographs were found to have masses corresponding to the expected values: 5943.2585 for 2'-O-Me *Cd9* T2 3' TFO and 5942.7873 for 2'-OMe *Cd9* T2 5' TFO (Table 2).

Thermal denaturation experiments were carried out as described above for the deoxyribo-TFOs. A representative melting curve is shown in Figure 6. The black curve represents melting of the duplex into single stands and the red curve shows melting of the third strand from the triplex. In contrast to the melting curve of the triplexes formed by the deoxyribo-TFOs, there is only one transition in the melting curve of the triplex

formed by the 2'-O-methylribo-TFO (Fig. 6). This single transition suggests that the third strand and duplex melt at the same temperature, which occurs at a temperature higher than that of the duplex alone. At pH 7.0, 2'-O-Me *Cd9* T2 3' TFO had a  $T_m$  of 76°C and 2'-O-Me *Cd9* T2 5' TFO had a  $T_m$  of 70°C (Table 2). At pH 7.5, the  $T_m$  decreased, with the  $T_m$  of 68°C for 2'-O-Me *Cd9* T2 3' TFO and a  $T_m$  of 61°C for 2'-O-Me *Cd9* T2 5' TFO (Table 2).

Gel electrophoretic mobility shift assays were performed as described above to assess the cross-linking efficiencies of the 2'-O-Me-Pt-TFOs targeted to the *Cd9* gene. The cross-linking experiments were performed in triplicate, and the results presented in Table 2. Under the experimental conditions and at pH 6.0, 32% of *Cd9* T2 3' Pt-TFO and 40% of 2'-OMe *Cd9* T2 5' Pt-TFO cross-linked to the target duplex DNA (Table 2). In contrast to the behavior of the deoxyribo-Pt-TFOs, significant levels of cross-linking were observed at pH 7.0 and pH 7.5. At pH 7.0, 35% of *Cd9* T2 3' Pt-TFO and 63% of 2'-OMe *Cd9* T2 3' Pt-TFO cross-linked to the target DNA (Table 2). At pH 7.5, 33% of 2'-O-Me *Cd9* T2 3' Pt-TFO and 40% of 2'-O-Me *Cd9* T2 5' Pt-TFO cross-linked to the target DNA (Table 2).

### **2.3 Fluorescein-Derivatized 2'-O-Me-Pt-TFOs**

Fluorescein-derivatized Pt-TFOs were prepared for use in live cell imaging by fluorescence microscopy to monitor localization of the oligonucleotide in the cells. A 5'-FITC-labeled 2'-O-Me *Cd9* T2 3' TFO having the same nucleotide composition and sequence as the 2'-O-Me *Cd9* T2 3' TFO was synthesized for studies in cultured cells (Table 1). A previously synthesized fluorescein labeled scrambled 3' TFO with similar

nucleotide composition as *Cd9* T2 3' TFO but slightly greater length was used as a positive control in the cell culture experiments (Table 1).

To determine the efficiency of binding and cross-linking of the FITC-labeled 2'-OMe *Cd9* T2 3' TFO, thermal denaturation and electrophoretic mobility shift assays were performed with both FITC labeled 2'-O-Me *Cd9* T2 3' TFO and the FITC labeled 2'-O-Me scrambled 3' TFO and their platinated derivatives..

The results of the binding assay are shown in Figure 7A. At pH 7.0, FITC-labeled 2'-O-Me *Cd9* T2 3' TFO had a  $T_m$  of 74°C, whereas the FITC-labeled scrambled 3' TFO had a  $T_m$  of 20°C (Fig. 7A). However, platination with inert platinum decreased the thermal stability of FITC- labeled 2'-O-Me *Cd9* T2 3' Pt-TFO to 67°C whereas the stability of FITC labeled 2'-O-Me scrambled 3' PT-TFO increased to 33°C (Fig. 7A).

To determine whether the active platinated scrambled TFO could react with the target duplex, 100 pmol of Pt- FITC-labeled scrambled 2'-OMe 3' Pt- TFO was incubated with the *Cd9* T2 3' target DNA and the results were analyzed by gel electrophoresis under denaturing conditions. Similar experiments were performed for the 2'-O-Me *Cd9* T2 3' Pt-TFO and FITC labeled 2'-OMe *Cd9* T2 3' Pt-TFO. The extent of cross-linking was determined from the relative intensities of the bands resulting from triplex formation. As shown in Figure 7B, triplex formation is only observed in the presence of the 2'-O-Me *Cd9* 3' Pt-TFO and FITC labeled 2'-O-Me *Cd9* T2 3' Pt-TFO. 26%, 26% and 31% of FITC-labeled 2'-OMe *Cd9* specific Pt-TFO cross-linked to the purine strand of the DNA target at pH 6.0, 7.0 and 7.5 respectively. For the FITC-labeled *Cd9* T2 3' Pt-TFO, the cross-linking efficiencies were similar,

24%, 27% at pH 6.0 and 7.0 respectively, except at pH 7.5, where it decreased slightly to 21% (Fig. 7B).

### **3. Uptake of Fluorescein-Derivatized 2'-O-Me-Pt-TFOs by NIH3T3 Cells in Culture**

To assess the cellular delivery of an inert-Pt-TFO (TFO conjugated with a chemically inactive form of the transplatin which does not interact with and cross-link to the target DNA duplex) and its localization in the cell, NIH3T3 cells were transfected with 678 pmoles of FITC labeled 2'-OMe *Cd9* T2 3' inert Pt-TFO in 2mL/well using either Lipofectamine<sup>TM</sup> 2000 and FuGENE HD respectively; fixed with PBS; and stained with Hoechst, a dye that stains nucleic acids and only fluoresces when it binds to the major groove of the duplex DNA (Adolf, Aschberger, & Pelster, 2013).

The live cells were examined by fluorescence microscopy. Three different fields of cells were examined in each experiment. The uptake efficiency was estimated by calculating the ratio of the cells exhibiting green fluorescence from the inert Pt-TFO to those exhibiting blue fluorescence from the Hoechst staining of DNA. The green fluorescence thus signals cells that have taken up the inert Pt-TFO, whereas the blue fluorescence represents the total number of cells in the field of view. Representative images are shown in Figure 8. In Figure 8A, the phase contrast image of the cells is in Panel 1, cells that have taken up the inert Pt-TFO are shown in Panel 2, the total number of cells as indicated by Hoechst staining are shown in Panel 3 and Panel 4 shows the image of Panel 2 merged with Panel 3.



A significant number of cells take up the inert Pt-TFO. Approximately 79% of the cells took up the inert Pt-TFO when complexed with Lipofectamine™ 2000, whereas a slightly higher percentage of the cells, 84%, took up the inert Pt-TFO when complexed with FuGENE HD (Fig. 8A). Examination of the cells at 40x magnification revealed that the inert Pt-TFO was mainly localized in the nucleus. As shown in Figure 8B, inert Pt-TFOs transfected using Lipofectamine™ 2000 were primarily localized in the nucleus, whereas in the cells transfected with FuGENE HD, the FITC-labeled TFOs were found to be distributed in the nucleus and cytoplasm.

#### **4. Effect of *Cd9*-Specific 2'-O-Me-Pt-TFO on *Cd9* mRNA and CD9 protein levels in NIH3T3 Cells**

##### **4.1 RT-qPCR Assays**

Preliminary RT-qPCR experiments were carried out to determine the effect of the 2'-OMe *Cd9* specific Pt- TFO on gene expression in NIH3T3 cells. In these experiments we used the m*Cd9* primers described by Huang et al. (Huang et al., 2011) to monitor *Cd9* mRNA levels and m*Gapdh* primers (Spandidos et al., 2010) to monitor glyceraldehyde-3-phosphate dehydrogenase (*Gapdh*) mRNA levels. GAPDH is a housekeeping gene that is commonly used in qPCR protocols to normalize for differences in mRNA recoveries in RT-qPCR experiments (Radonić et al., 2004). The RT-qPCR assays were optimized to achieve increased sensitivity specificity and reproducibility over a dynamic linear range. One of the most common methods of optimizing RT-qPCR reactions is to perform the assay on serial dilutions of the cDNA

and plot the cycle threshold (Ct) values against the log of the cDNA concentrations to obtain a standard curve. The sequences and product size of the m*Cd9* (mouse *Cd9*) primer (Huang et al., 2011) and m*Gapdh* (mouse *Gapdh*) primers (Spandidos et al., 2010) used in the RT-qPCR are shown in Table 3. Three replicates were run for each dilution, over a 5-fold dilution range. Figure 9A is the plot of the standard curve. Several criteria define the characteristics of the standard curve. For an effective protocol, the slope of the standard curve should be between -3.2 and -3.5, as a 100% efficient assay will result in a standard curve with a slope of -3.3 (Nolan et al., 2006). Additionally, the  $R^2$  value is used to measure the reproducibility of the assay and is expected to be  $>0.98$  to indicate that the assay is reliable and reproducible. The slopes and efficiency of the target and the housekeeping primers should be similar as this indicates similar sensitivity (Nolan et al., 2006). This is important as data obtained from the RT-qPCR reaction is normalized to the endogenous housekeeping gene to internally control for errors in the protocol (Nolan et al., 2006). In Figure 9A, the slope for *Cd9* is -3.1035 with an  $R^2$  of 0.99692, an efficiency of 109.99% and the slope for *Gapdh* is -3.288,  $R^2$  of 0.99768, which translates into an efficiency of 101.40%.

One way to determine the quality of the RNA transcript and the RT-qPCR protocol is to run the products on an agarose gel. Figure 9B shows the products of the RT-qPCR reactions run on an agarose gel. As can be seen, there are no degraded or truncated RNA products and the products of *Cd9* II and *Gapdh* I are of the correct size, 208 kb and 123 kb respectively (Table 3).

To analyze the effect of the *Cd9* T2 3' Pt-TFO on the *Cd9* mRNA level, NIH3T3 cells were transfected with Pt-TFO using either FuGENE HD or

Lipofectamine<sup>TM</sup> 2000 at a total concentration of 0.7 nmol/dish and harvested 72 hours or 48 hours post transfection respectively. Total RNA was extracted from the cells and RT-qPCR was used to analyze the *Cd9* mRNA transcript levels using *Cd9*-specific primers, with *Gapdh*-specific primers used as a control. The levels of mRNA expression were measured using the cycle threshold (Ct). The relative fold change in expression was calculated using the  $2^{\Delta\Delta Ct}$  method (Livak & Schmittgen, 2001) where the average of delta Ct values for the *Cd9* mRNA was normalized to that of *Gapdh* mRNA control and compared to untreated control cells to control for any internal variations in the RT-qPCR.

The results are shown in Figure 10. These data are representative of two independent experiments performed in triplicate. Vertical bars represent the standard deviation from the mean for the two replicates. For transfection with FuGENE, the FITC scrambled 3' Pt-TFO mRNA expression was 86% ( $\pm 0.25$ ) of the untreated cells, and the FITC *Cd9* 3' Pt-TFO mRNA expression was 94% ( $\pm 0.25$ ) of the untreated cells (Fig. 10). For transfection with Lipofectamine<sup>TM</sup> 2000, the control FITC labeled scrambled 3' Pt-TFO mRNA expression was 68 % ( $\pm 0.05$ ) of the untreated cells, and the FITC-labeled *Cd9* 3' Pt-TFO mRNA expression was 71 % ( $\pm 0.06$ ) (Fig. 10).

## 4.2 Western Blot Analysis

A Western blot was used to determine if the changes observed in the mRNA after Pt-TFO treatments were also reflected in the CD9 protein level. The cells were transfected with FITC labeled scrambled Pt-TFO and FITC labeled *Cd9* T2 3' Pt- TFO as previously described. The cells were lysed and the whole cell lysate was subjected to

SDS-PAGE followed by western blotting. Beta-actin was used as a loading control. The blot was analyzed by ImageJ. The ratio of CD9 expression to beta-actin expression were determined using Image J (NIH). All CD9 protein levels were first normalized to beta-actin protein expression levels to control for variation in loading. The results were then expressed as a percentage of the level of control cells. The blot is shown in Figure 11A and the quantitative analysis presented in the bar graph in Figure 11B. The level of CD9 protein in cells transfected using FuGENE HD were comparable in FITC-labeled scrambled 3' Pt-TFO (97% of CD9 protein in untreated) and FITC-labeled *Cd9* 3' Pt-TFO (95% of CD9 protein in untreated) treated cells (Fig.11B). Similar results were obtained for cells transfected using Lipofectamine<sup>TM</sup> 2000 reagents where the CD9 protein levels were comparable in cells transfected with FITC-labeled scrambled Pt-TFOs (100% of CD9 proteins in untreated) and cells transfected with FITC-labeled *Cd9* T2 3' Pt-TFOs (90% of CD9 protein in untreated) (Fig.11B).

For the RT-qPCR and western blotting analyses, the statistical significance (p-value) was not calculated as each experiment was only repeated once.

## DISCUSSION

Triplex-forming oligonucleotides (TFOs) react with their target DNA in a sequence specific manner to inhibit gene expression, an approach that makes them attractive as tools for selectively manipulating the activity of genes. The overall goal of this thesis project was to investigate the possibility of using triplex forming oligonucleotides to inhibit expression of genes that are important for the maturation or fertilization of oocytes in a mouse cell culture model system. The specific aims of the project included the identification of TFO binding sites in the target genes, characterizing the interactions of the TFO with short DNA duplexes that contain the TFO binding sites, investigating the uptake of the fluorescein-derivatized TFOs by mouse NIH3T3 cells in cell culture using fluorescence microscopy and examining the ability of the platinated TFOs to inhibit gene expression in mouse NIH3T3 cells using RT-qPCR and western blot techniques.

The three target genes studied were *Cd9*, *Plk1*, and *Cdc25b*. We used a web-base search engine (Gaddis et al., 2006) to screen the three genes for potential TFO binding sites. The following criteria were used in this search: minimum TFO length of 15 nucleotides, low cytosine content, no contiguous cytosine sequences, and a maximum of one pyrimidine interruption. Theoretically, these criteria should identify TFOs that can form triplexes with their target DNA duplexes, however, biophysical and biochemical studies are performed to characterize the interaction of the TFOs and Pt-TFOs with their DNA targets.

## 1. Interactions of TFOs and Pt-TFOs with DNA Duplexes

### 1.1.a Deoxyribose-TFOs and Deoxyribo-Pt-TFOs

As can be seen from the results, the thermal stabilities of the triplexes formed by deoxyribo-TFOs seem to be dependent on length and cytosine content of the TFO sequence. For example, triplexes formed by *Cd9* T3 3' TFO and *Cd9* T3 5' TFO had higher slightly higher  $T_m$ s than those formed by *Cd9* T2 3' and 5' TFO targets (19 nucleotides and 21% cytosine content compared to 18 nucleotides and 27.7% cytosines respectively). This is consistent with observations in previous studies where TFOs with longer nucleotide sequence and lower cytosine content tend to form more stable triplexes (Campbell & Miller, 2009a; Crooke, 1992; Graham & Miller, 2012). However, an exception to this observation is the *Cd9* T1 3' TFO and *Cd9* T1 TFO 5' TFO, which despite the 18 nucleotide length and 50% cytosine content, had  $T_m$ s of 42°C and 45°C respectively. Similarly, both *Cdc25b* T1 3' and 5' TFOs are 17 nucleotides in length with 35% cytosine content, but the 3' TFO had lower  $T_m$  (23°C) than the 5' TFO (34°C). While this might suggest that a 5' terminal guanine provides more stability than a 3' terminal guanine, these differences vary for almost all the targets. All these observations suggest that several factors, in addition to nucleotide length, cytosine content, and position of the terminal guanine in the TFO, might be involved in defining the stability of triplexes formed by the TFO. In support of this notion, Graham et al (2012) have shown that sequences flanking the TFO binding site can affect TFO binding affinity (Graham & Miller, 2012).

The extent of cross-linking by deoxyribo-Pt-TFOs is dependent on pH. At pH 6, all of the deoxyribo-Pt-TFOs cross-linked at pH 6 with different efficiencies (Fig. 5B).

However, as the pH increased, the extent of cross-linking decreased dramatically. The absence of triplex formation at pH 7.0 by *Plk1*-3' Pt-TFO, *Cdc25b* T1 3' Pt-TFO, *Cdc25b* T1 5' Pt-TFO, *Cdc25b* T2 3' Pt-TFO, *Cdc25b* T2 5' Pt-TFO imply that while these Pt-TFOs are capable of binding to their target duplexes, their triplex formation occurs at  $T_m$  lower than the experimental conditions (37°C), which suggest that inefficient binding interactions under the experimental conditions do not favor cross-linking with the target DNA (Fig. 5b). An exception to this is *Cd9-2* 3' & 5' Pt-TFO, whose 3' and 5' terminal guanines are both platinated. Despite its  $T_m$  above the experimental condition of 37°C, it did not cross-link to its target DNA, though it was assumed that the double platination would increase the cross-linking efficiency.

In addition, it was observed that at pH 6, all deoxyribose 5' Pt-TFOs cross-linked at higher efficiency than 3' Pt-TFOs. While this may suggest that the platinum on the 5' terminus of the TFO increased its cross-linking efficiency, this pattern of cross-linking was not observed at pH 7, where the cross-linking was highly variable despite similarities in  $T_m$  for both 3' and 5' TFOs of each target DNA. With this variable cross-linking at different pH conditions, it is difficult to conclusively determine any specific relationship between the terminal platination and cross-linking efficiency. Additionally, previous experiments performed by Graham and Miller (2012) suggested that 3'-platination gave higher levels of cross-links as opposed to 5'-

platination (Graham & Miller, 2012)., lending support to the idea that the efficiency of the cross-linking is determined in some as-yet not understood way dependent upon the sequences flanking the TFO binding site.

### 1.1.b 2'-OMe TFOs and Pt-TFOs

As previously observed with the deoxyribo-TFOs, the  $T_m$ s of 2'-OMe TFOs were also dependent on pH as the  $T_m$  decreased with increasing pH. However, as expected the  $T_m$ s of the triplexes formed by 2'-OMe *Cd9* T2 3' TFO and *Cd9* T2 5' TFO were on average about 30 °C higher than those of the corresponding deoxyribo-TFOs under all experimental conditions tested (Fig. 4B, Table 2). In addition, the  $T_m$  of the triplex formed by 2'-OMe *Cd9* T2 3' TFO was slightly higher than that of the triplex formed by 2'-OMe *Cd9* T2 5' TFO.

On average, at pH 7, the cross-linking efficiencies of the 2'-OMe Pt-TFOs were higher than their deoxyribo- Pt-TFO counterparts (Fig. 5B and 7B) In contrast to the deoxyribo-TFO studies, results from the 2'-OMe Pt-TFO cross-linking experiments show that the extent of cross-linking is independent of pH. Thus 2'-OMe *Cd9* T2 3' Pt-TFO had similar cross-linking efficiencies over the pH range of 7.0 to 7.5 (Table 2). Similar results were observed for Pt-2'-OMe *Cd9* T2 5' TFO. This pH independent cross-linking efficiency is a result of the substitution of the cytosines in the deoxyribo-TFO with 5-methylcytosines increases triplex stability, significantly reducing the pH dependency of the triplex formation as they obliterate the requirement for C protonation to allow the triplex formation to occur.



As both 2'-OMe *Cd9* T2 3' Pt-TFO and 2'-OMe *Cd9* T2 5' Pt-TFO have the same nucleotide composition and length (19 nucleotides), and target the same sequence in the first intron of the *Cd9* gene (Fig. 2a) any differences in triplex  $T_m$  and cross-linking efficiency could be due to the terminal guanines. Both of the 3' and 5' Pt-TFOs bind and cross-link to the same sequence in the target DNA. The Pt-TFO with the 5' terminal guanine is more effective at cross-linking with the target DNA though this observation is in contrast with observations made by Graham et al (2012). (These are 2'-OMe and they have  $T_m$  in the 60s, higher than the 37 °C of the cross-linking experimental condition). They observed that TFOs with a 3'-platinum group cross-link more efficiently than TFOs of the same sequence with a 5'-platinum (Graham & Miller, 2012). This indicates that other factors such as the sequence of the TFO, neighboring sequences of the DNA target sequence among others contribute to the cross-linking efficiency of the Pt-TFO to its target.

In summary, the  $T_m$  values of 2'-OMe *Cd9* T2 3' TFO and *Cd9* T2 5' TFO were at least 30 °C higher than their corresponding deoxyribose-TFOs and as a consequence their platinum derivatives cross-link with higher efficiency. This increase in  $T_m$  and extent of cross-linking is an effect of the stability conferred by, 2'-O-methyl and 5' methylcytosine modifications. These findings are in agreement with the work of Graham et al, (2012) and Campbell et al (2009) who demonstrated that modification of the TFO with 2-O-methylribose nucleotides increased the binding stability and cross-linking efficiency of the TFO. Overall, the studies of the interactions of the TFOs and Pt-TFOs with DNA duplexes is consistent with previous studies that showed 2'-O-

methyl and 5' methylcytosine modifications of the TFO decreases the pH dependency of the triplex formation (Maher et al., 1989) and stabilizes the triplex formation (Campbell & Miller, 2009a; Escudé et al., 1992; Graham & Miller, 2012; Knauert & Glazer, 2001b; Xodo et al., 1991).

### 1.1.c Fluorescein-Derivatized 2'-OMe-Pt-TFOs

Prior to performing cellular uptake and in vivo studies of the TFO biological activities, FITC-labeled 2'-OMe *Cd9 T2 3'* TFO was synthesized to make it easier to track the TFO by live cell fluorescence microscopy. We characterized the interactions of the fluorescein-derivatized 2'-OMe- inert-Pt-TFO with the target DNA duplex using UV thermal denaturation and EMSA. Similar experiments were performed using a scrambled 3' Pt-TFO obtained from Mindy Graham, which has a similar nucleotide composition to that of *Cd9 T2 3'* TFO (Table 1). Both the FITC-labeled 2'-OMe *Cd9 T2 3'* TFO and its inert platinum derivative formed stable triplexes with the *Cd9T2* DNA. The triplex formed by FITC-labeled 2'-OMe *Cd9 T2 3'* TFO had a  $T_m$  similar to that of unlabeled 2'-OMe *Cd9 T2 3'* TFO (74°C and 76°C respectively), suggesting that the FITC label does not affect the binding interactions of the TFO with the target DNA (Fig. 7A). However, Platination of the FITC labeled 2'-OMe *Cd9 T2 3'* TFO decreases the  $T_m$  of the triplex to 67°C (Fig. 7A). In contrast, while the FITC-labeled scrambled control TFO and its derivatized platinum counterpart formed stable triplexes with reasonably high  $T_m$ s, they were lower than that of the FITC-labeled 2'-OMe *Cd9 T2 3'* TFO (Fig. 7A).

EMSA results indicate that FITC-labeled 2'-OMe *Cd9* T2 3' Pt-TFO cross-links with similar efficiency to the target DNA as the unlabeled 2'-OMe *Cd9* T2 3' Pt-TFO at pH 6 and 7, in support of the previous observation that the FITC label does not affect the interactions of the TFO with the target as expected, the FITC-labeled scrambled 3' Pt-TFO did not cross-link to the *Cd9* T2 DNA target at any of the pH conditions tested (Figure 7B).

## **2. Uptake of Fluorescein-Derivatized 2'-OMe-Pt-TFOs by NIH3T3 Cells in Culture**

To assess the uptake of the fluorescein-derivatized 2'-OMe Pt-TFOs, NIH3T3 mouse fibroblast cells were transfected with the FITC-labeled 2'-OMe *Cd9* 3' inert Pt-TFO. The cellular delivery and uptake efficiencies were determined by fluorescence microscopy. As shown in Figure 8A, the Pt-TFOs were successfully transfected into the mouse NIH3T3 cells. Higher uptake efficiency was observed with Pt-TFOs complexed with FuGENE HD than Pt-TFOs complexed with Lipofectamine<sup>TM</sup> 2000 (Fig 8A). The merge of the images of cells in Panel 4, comprising images of cells that have taken up the FITC- labeled TFO (Panel 2) and images of cells whose DNA is stained with Hoescht of DNA (Panel 3), show that the TFO is in the nucleus (Fig. 8B). Observation at higher magnification (40x) shows increased nuclear localization was observed when transfection was carried out using Lipofectamine<sup>TM</sup> 2000 compared to transfection using FuGENE HD (Fig. 8B). However Lipofectamine induced higher cytotoxicity (data not shown) compared with FuGENE HD. In summary, cells transfected with inert Pt-TFO complexed with FuGENE HD expressed high uptake efficiency and lower cytotoxicity, although nuclear localization was suboptimal. In

contrast, uptake of inert Pt-TFO complexed with Lipofectamine™ 2000 was slightly lower although nuclear localization was higher. These differences in uptake efficiencies and localization could affect the ability of the Pt-TFO to inhibit CD9 expression in the cells.

### **3. Effect of *Cd9*-Specific 2'-O-Me-Pt-TFO on *Cd9* Expression in NIH3T3 Cells**

The effects of FITC-labeled 2'-O-Me- *Cd9* T2 3' Pt-TFO and FITC-labeled 2'-O-Me-scrambled Pt-TFO on *Cd9* mRNA and protein levels were determined in mouse NIH3T3 cells in culture.

#### **3.1.a RT-qPCR Assays**

RT-qPCR was used to assess the levels of CD9 mRNA in cells treated with FITC-labeled 2'-O-Me- *Cd9* T2 3' Pt-TFO and FITC-labeled 2'-O-Me-scrambled Pt-TFO. The *Cd9* mRNA levels are normalized to the mRNA levels of Gapdh. Preliminary experiments showed that FuGENE HD complexes of the FITC labeled 2'-OMe *Cd9* T2 3' Pt-TFO or the FITC-labeled scrambled TFO failed to suppress *Cd9* mRNA levels in the NIH3T3 cells. In contrast, Lipofectamine complexes of FITC-labeled 2'-OMe *Cd9* T2 3' Pt-TFO or FITC-labeled 2'-OMe scrambled Pt-TFO inhibited *Cd9* mRNA levels by 29% and 32% respectively.

These results show a tentative correlation between the delivery of the TFOs to the nucleus and the effect of the TFOs on *Cd9* mRNA levels. However, because both the FITC labeled 2'-OMe scrambled control Pt-TFO and the FITC-labeled 2'-OMe *Cd9* T2 3' Pt-TFO inhibit *Cd9* mRNA levels, we cannot conclude that the inhibitory effect

observed is a consequence of specific interaction of the 2'-OMe *Cd9*T2 3' Pt-TFO with the *Cd9* gene.

### **3.1.b Western Blot Assays**

If the TFO is able to inhibit transcription of the *Cd9* gene, it would be expected to reduce CD9 protein levels. Western blot analysis of CD9 protein expression showed that the protein level in cells transfected with FITC-labeled 2'-OMe scrambled 3' Pt-TFO or FITC *Cd9* 3' Pt-TFO using both FuGENE HD or Lipofectamine<sup>TM</sup> 2000 transfection reagent did not change (Fig. 11). These results suggest that if TFO-mediated inhibition of *Cd9* gene transcription had occurred it was not sufficient to significantly affect CD9 protein expression.

## **4. Summary of the effect of *Cd9*-Specific 2'-O-Me-Pt-TFO on *Cd9* Expression in NIH3T3 Cells**

In analyzing the results of the experiments described above it is clear that despite the high binding affinity of the *Cd9* TFO for its target in vitro and its ability to cross-link to its target DNA sequence when platinated, the platinated TFO did not inhibit *Cd9* gene expression in a sequence specific manner.

Previous studies suggest that TFOs that do not cross-link to their DNA targets are highly prone to displacement by transcriptional machinery of the cell and have limited or transient inhibitory effects (Colombier et al., 1996; Young et al., 1991). Based on the assumption that intracellular activity of TFOs requires the TFO to bind and cross-link to its target, we might expect the FITC labeled *Cd9* T2 3'Pt-TFO to

have a minimal effect on gene expression. According to our EMSA experiments, approximately 25% of the FITC labeled 2'-OMe *Cd9* T2 3' Pt-TFO cross-linked to its target DNA under physiological conditions in vitro. It seems unlikely that more extensive cross-linking to genomic DNA would be achieved in the cells for several reasons: (1) The micromolar concentrations required for efficient cross-linking in vitro may not be attained in the nucleus of the cell; (2) The TFO binding site may not be accessible to the TFO due to association with histones or other DNA binding proteins; and (3) The platinumium may become inactive because of reaction with other molecules, such as glutathione, while in the intracellular environment.

We also observed substantial inhibition of gene expression observe in cells treated with the FITC-labeled scrambled control Pt-TFO. As discussed in the previous section, this platinated TFO does not cross-link with the *Cd9* DNA target in vitro (Fig.7). The observed inhibition may therefore be due to off-target effects.

Such effects by TFOs have been reported by others (Kim et al., 1998; Morvan et al., 1993) and one report suggested that TFOs may exhibit non-sequence-specific activity through interactions with DNA polymerase (Morvan et al., 1993). Alternatively the scrambled Pt-TFO may interact with other homopurine tracts in the genome. A quick nucleotide blast of the scrambled TFO sequence against the mouse genomic and transcript database using the NCBI BLAST (Basic Local Alignment Search Tool (BLAST) program identified similar sequences in different transcripts and genes, the most significant of which was the mouse general transcription factor II I (*Gtf2i*) (<http://blast.ncbi.nlm.nih.gov/Blast.cgi>) (Query id: ICI21473, molecule type: nucleic acid, query length-19, in mouse genome). There was a 100% sequence match with 18

nucleotides in several variants of the *Gtf2i* transcription factor. Given the sequence similarities, it is possible that the scramble Pt-TFO can interact with non-target sequences such as the one found in the gene of this transcription factor and consequently inhibit overall gene transcription. Investigating the effect of the scrambled Pt-TFO on expression of other genes could provide more insights into the potential off-target effects of this scrambled sequence.

## **5. Proposed changes to research protocols**

In the case of the *Cd9*-specific Pt-TFO, there does not appear to be a strong correlation between its ability to cross-link to its target DNA and its biological activity in vivo. To fully elucidate the inhibitory effects of the *Cd9* T2 3' Pt-TFO, several changes to the current research methods are proposed. These include changes in the experimental protocols used to select TFOs and Pt-TFOs that can interact with the target DNA duplexes, selection of scrambled Pt-TFOs as positive controls in RT-qPCR and western blot techniques, making changes to the reference genes used in the RT-qPCR protocols, exploring alternative methods of cellular delivery of TFOs and investigating the effects of the *Cd9* T2 5' Pt-TFO.

### **5.1.a Changes in experimental protocols used to select TFOs and Pt-TFOs**

The results, while preliminary, suggest that there is some correlation between in vivo and in vitro results as observed (for Lipofectamine-Pt-TFO complexes), a question remains about its sequence specificity as similar results were obtained with scrambled Pt-TFO. The FITC- label on the *Cd9* T2 3' Pt-TFO did not significantly

change its binding stability or ability to form adducts with its target DNA duplex. Differences observed could indicate that the in vitro experimental conditions do not reflect the complexities of the intracellular compartment of the cell. Therefore it is important that the specificity of TFO interactions with genomic DNA in cell culture should be considered. This is because the TFO interactions with cellular components such as proteins, and transcriptional proteins may all affect its intracellular activity. To examine the sequence specific interactions of the Pt-TFO with the target DNA, it might be worthwhile to develop an assay to see if the Pt-TFO reacts with cellular genomic DNA. This approach is currently being pursued Mindy Graham in our lab

#### **5.1.b Selection of scrambled Pt-TFOs as positive controls in RT-qPCR and western blot techniques**

These experimental studies stress the need for proper experimental controls to accurately analyze the effect of the Pt-TFOs on target gene expression. A scrambled control is important for validating any effect observed when the cells are treated with Pt-TFOs. Our scrambled Pt-TFO positive control did not work for our experiments as it failed to correlate lack of triplex formation in vitro with the observed biological activity in vivo. Ideally, the best control is a scrambled version of target TFO that affect the triplex stability but not the gene expression. Mahato et al. (2005) in their review noted that it may be difficult to design scrambled controls for polypyrimidine TFOs targeted to endogenous genes, as opposed to target genes inserted in plasmids (Mahato et al., 2005), though the authors did not provide an explanation for their observation. As the nucleotide BLAST results indicate, it is nearly impossible to find a scrambled sequence



that does not have at least partial complementarity to non-targeted genes. A better approach would be to use the inert platinum version of the gene-specific TFO, which would not be able to cross-link to its target and would be expected to give little or no inhibition.

### **5.1.c Changes to the reference genes used in the RT-qPCR protocols**

Reliable and consistent comparative studies using RT-qPCR depends on the use of reference genes that are minimally affected by treatment conditions. For our assays we used *Gapdh* because it is a common housekeeping gene. However, the consensus regarding the utility of *Gapdh* is sharply divided, with some studies presenting evidence in support of it (Gorzelnik, Janke, Engeli, & Sharma, 2001; Raaijmakers, van Emst, de Witte, Mensink, & Raymakers, 2002) while others suggest that it varies considerably with treatments and is unsuitable as a reference gene for data analysis (Glare, Divjak, Bailey, & Walters, 2002; Radonić et al., 2004; Zhong & Simons, 1999). Several alternatives are available, including beta actin, RNA polymerase, 18s gene. However, as these genes are potentially susceptible to various experimental conditions to a degree, using a combination of reference genes could generate more reliable and reproducible data set (Radonić et al., 2004). We performed comparative studies of a few reference genes and found that the results vary with each reference gene (data not shown). Hence for future studies, combinations of reference genes should be used in the RT-qPCR to make quantitative analysis of results more accurate.

### **5.1.d Exploring alternative methods of cellular delivery of TFOs**

As previously discussed, the ability of Pt-TFOs to inhibit the expression of the target gene depends on their successful cellular delivery, nuclear localization and intracellular stability, underlying the significance of an efficient transfection reagent that delivers the Pt-TFOs to the nucleus. As our FuGENE HD RT-qPCR results demonstrate, delivery of Pt-TFO to the cytoplasm of the cell does not translate into efficient TFO inhibition of target gene. The Pt-TFOs have to be localized to the nucleus to interact with the endogenous DNA duplex.

Different transfection reagents will have different successes in cellular delivery of the TFO. For future experiments, the transfection protocol needs to be further optimized, as our uptake efficiencies were not high. In addition to optimizing the current transfection protocol, it is important to explore alternative cellular delivery mechanism such as conjugation to aptamers, or other commercially available chemical liposomal transfection reagents. There are variations of these chemical transfection reagents and it might be beneficial to evaluate a few more for their effectiveness.

Also, use of aptamers can also be explored. Aptamers are single-stranded DNA or RNA oligonucleotides that fold into unique 3D structures (Levy-Nissenbaum, Radovic-Moreno, Wang, Langer, & Farokhzad, 2008). Aptamers are able to bind to nucleic acid, proteins and sugars with high affinity, and have been adapted for specific cell delivery. This technology has been used to deliver siRNA to cells (FAU et al., 1229; Zhou J FAU - Rossi, John,J. & Rossi, 0714) and should be explored for cellular delivery of Pt-TFOs.

### **5.1.e Investigating the effects of the *Cd9* T2 5' Pt-TFO**

Results of the binding experiments and cross-linking experiments indicate that the 2' OMe *Cd9* T2 5' TFO has similar binding stability but increased cross-linking efficiency compared to that of 2'-OMe *Cd9* T2 3' TFO. In vivo analysis of the 2'-OMe *Cd9* T2 5' Pt-TFO effect on gene expression should be performed to determine if it can significantly inhibit the expression of the *Cd9* T2 target. Furthermore, a combination of TFOs each targeting different regions of the same gene could induce more pronounced inhibition of gene expression. Kim et al (1998) showed that co-transfecting HeLa cells with c-myc expressing luciferase reporter plasmid construct with two promoter regions, P1 and P2 respectively, targeted by two TFOs resulted in 90% inhibition of luciferase activity whereas neither TFO targeting P1 or P2 alone could significantly inhibit the luciferase activity (Kim et al., 1998). It would be worthwhile to transfect the NIH3T3 cells with both 2'-OMe *Cd9* T2 3' Pt-TFO and *Cd9* T2 5' Pt-TFO to determine if the combined Pt-TFOs can significantly inhibit *Cd9* gene expression.

## **6. Conclusion**

It is evident that the specific requirements of TFOs place several limitations on the number of target sequences amenable for triplex formation. However, nucleotide modifications make it possible to design TFOs capable of effectively interacting with their target DNAs under physiological conditions. The 2'-O-methylribo modification increases the stability of the triplexes formed by TFOs and the efficiency of cross-linking by Pt-TFOs.

Although the FITC-labeled *Cd9* T2 3' Pt-TFO demonstrated modest ability to inhibit the *Cd9* mRNA levels we were unable to demonstrate that this inhibition was a sequence specific effect of the TFO.

The results of our studies reveal some impediments to the biological applications of Pt-TFOs. Efficient transfection of the TFO is a necessary and critical requirement for TFO activity, and our results indicate that the uptake efficiency and nuclear localization differs for different transfection reagents. Hence effective transfection methods are needed. In addition to that, there is a need for an understanding of the intracellular activity of TFO as there seems to be a disconnect between the in vitro experimental results and the in vivo experimental observations, at least for our experiment. The in vivo applications of Pt-TFOs may require further understanding of the specific interactions of Pt-TFOs at the genomic level in cell cultures. Such understanding is also relevant to the design of better controls for our assays. For such reasons, we cannot completely disregard the potential of the *Cd9* TFOs to modulate the expression of the *Cd9* gene. As we develop better understanding, better techniques and optimized protocols, we may explore the full potential of these TFOs. Therefore we anticipate that these preliminary results will encourage further investigations aimed towards demonstrating the sequence specific cellular activity of the *Cd9* Pt-TFOs, an approach of great interest in oocyte biology research. Future investigations may include using RT-qPCR to select TFOs and Pt-TFOs capable of interacting with their target DNA duplexes, using multiple reference genes in the RT-qPCR, screening for more effective scrambled control, investigating the ability of the 2'-OMe *Cd9* T2 5' TFO to inhibit *Cd9* gene expression in vivo and

exploring other transfection strategies to study their effects on the in vivo antigenic effects of the *Cd9* TFOs.

**Table 1. Sequences of triplex forming oligonucleotides (TFO) and their corresponding DNA target duplex**

TARGET /TFO	Sequences	GenBank number	Chromosome region
<b>Plk1 T2 Duplex</b>  <i>Plk1</i> T2 3' TFO	5' d-GACACTTTCCTTGCCTTTTTTTTAGAT CTGTG <u>AAAGGAACGGAAAAAA</u> AATCTA-d 5'  GTTTCCTTGCCTTTTTTTT-d 5'	NC_00007 3.6	Chromosome 7- Intron 2
<b>Cdc25b T1 Duplex</b>  <i>Cdc25b</i> T1 3' TFO <i>Cdc25b</i> T1 5' TFO	5' d-AGGGCTTTCCTTCCCTTTTCACCT TCCCG <u>AAAGGAAGGAGAAAG</u> TGGA-d 5'  GTTTCTCCTTCCTTTTC-d 5' CTTTCCTTCCTTTTG-d 5'	NC_00006 8.7	Chromosome 2- Intron 11
<b>Cdc25b T2 Duplex</b>  <i>Cdc25b</i> T2 3' TFO <i>Cdc25b</i> T2 5' TFO	5' d-TGACTCTCTTGCTTCCTCTTTCCTGG ACTGAGAGAACGAAGGAGAAAGGACC-d 5'  GTCTCTTGCTTCCTCTTTC-d 5' CTCTCTTCCTTCCTCTTTG-d 5'	NC_00006 8.7	Chromosome 2- Intron 14
<b>Cd9 T1 Duplex</b>  <i>Cd9</i> T1 3' TFO <i>Cd9</i> T1 5' TFO	5' d-CAGGGAGGAGAGGAAAGGGAAGGCT GTCCCTCCTCTCCTTTCCCTTCCGA-d 5'  5' d-CTCCTCTCCTTTCCCTTG 5' d-GTCCTCTCCTTTCCCTTC	NC_00007 2.6	Chromosome 6- Intron 2
<b>Cd9 T2 Duplex</b>  <i>Cd9</i> T2 3' TFO <i>Cd9</i> T2 5' TFO <i>Cd9</i> T2 3'&5' TFO  <i>Cd9</i> T2 3' TFO <i>Cd9</i> T2 FITC 3' TFO	5' d- CAGAACTTCTTTCTCTCTTTTTCCTTTT  GTCTTG <u>AAGAAAGAGAGAGAAAAGGAAAA</u> -d 5'  GTTCTTTCTCTCTTTTT -d 5' TTCTTTCTCTCTTTTTG-d 5' GTTCTTTCTCTCTTTTTG-d 5'  GTTCTTTCTCTCTTTTT-mr 5' 6FAM-GTTCTTTCTCTCTTTTT-m 5'	NC_00007 2.6	Chromosome 6- Intron 1

<b>Cd9 T3 Duplex</b>  Cd9 T3 3' TFO Cd9 T3 5' TFO	<b>5' d-</b> <b>GCAGACTTTCTTTTTCTTTCTTCTCTCTTC</b>  <b>CGTCTGAAAGAAAAGAAAGAAGAGAGAA</b> <b>G-d5'</b>  GTTTCTTTTTCTTTCTTCT -d 5' TTTCTTTTTCTTTCTTCTG-d 5'	<b>NC_00007</b> <b>2.6</b>	<b>Chromosome 6-</b> <b>Intron 2</b>
<b>Cd9 T6 Duplex</b>  Cd9 T6 5' TFO	<b>5'd-CTCAATTC</b> <b>TTTTCTTTCTTTTTGGAGG</b>  <b>GAGTTAAGAAAAGAAAGAGAAAACCTCC-d</b> <b>5'</b>  TTCTTTTCTTTCTTTTTG-d 5'	<b>NC_00007</b> <b>2.6</b>	<b>Chromosome 6-</b> <b>intron 1</b>
Scrambled 3' TFO	GTTTTT <u>CCCCC</u> TTTTTTT-6FAM-mr 5'	<b>N/A</b>	<b>N/A</b>

Key: **d**, deoxy nucleotide, **mr**, 2' o-methyl modified nucleotides and C, 2'-0-methyl-methylcytosine; Plk1 –Polo-like Kinase 1 (drosophila); *Cdc25b*-Cell division cycle 25 homolog B (*S. cerevisiae*); *Cd9-Cd9* antigen

**Table 2. Melting temperature and electrophoretic mobility shift assay (cross-linking) of 2'-0-methylribonucleotides *Cd9* T2 3' and 5' TFO.** Melting Temperatures of the third strand of the triplex formed by 2'-0-methyl *Cd9* T2 3' and *Cd9* T2 5' TFO in pH 7.0 and pH 7.5 triplex buffers. Cross-linking between platinated *Cd9* 3' TFO and *Cd9* 5' TFO and their respective DNA duplexes. Solutions containing 1  $\mu$ M  $^{32}$ P-labeled DNA duplex and either 0, 1, 5 and 10  $\mu$ M of Pt-*Cd9* 3' TFO, Pt-*Cd9* 3' TFO were incubated in pH 6, pH 7, pH 7.5 triplex buffers for 24 h at 37°C and the reaction mixtures were analyzed by electrophoresis on denaturing 20% polyacrylamide gel. Percent cross-linking of Pt-TFO were determined by phosphoimaging. Dash arrow denotes the triplex and solid arrow denotes the Duplex. Masses of oligonucleotides were determined by mass spectrometry.

**Table 2: Melting temperature and electrophoretic mobility shift assay (cross-linking) of 2'-0-methylribonucleotides *Cd9* T2 3' and 5' TFO**

2'-0-methylribose TFO	Tm (°C)		Crosslinking			Mass	
	pH 7.0	pH 7.5	pH 6.0	pH 7.0	pH 7.5	Expected Mass	Observed Mass
CD9 3' TFO	76	68	32	35	33	5944.11	5943.2585
CD9 5' TFO	70	61	40	63	40	5944.11	5942.7873



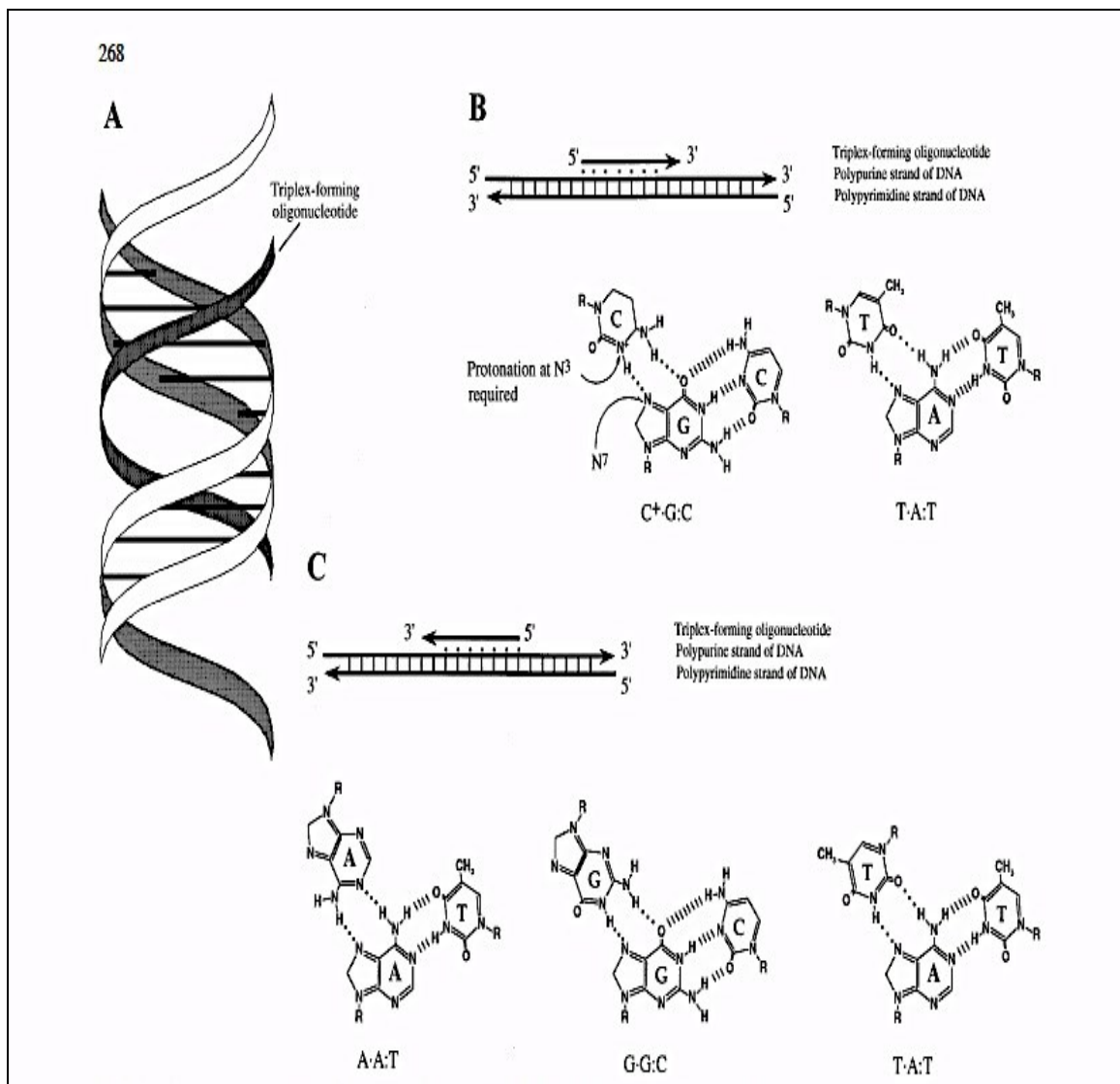
**Table 3. Primer sequences used in RT-qPCR**

Short name	Full name	GenBank Number	Product size	Primers
mCd9	Cd9 antigen	NM_007657	208kb	Forward (5'-3') CTGGCATTGCAGTGCTTGCTA  Reverse (5'-3') AACCCGAAGAACAATCCCAGC
mGAPDH	Glyceraldehyde-3-phosphate dehydrogenase	NM_008084	123kb	Forward (5'-3') AGGTCGGTGTGAACGGATTG  Reverse (5'-3') TGTAGACCATGTAGTTGAGGTC A

\*mCD9 primer sequences were taken from Huang et al (2011).

**Figure 1: Triplex formation by TFO interaction with a DNA duplex. (A)** A third strand (polypurine tract labeled in figure) binds to the major groove of the target DNA helix to form the triplex. **(B)** Triplex binding motifs -base triads of triplexes formed either through parallel Hoogsteen (C: G: C or T: A: T) or **(C)** antiparallel reverse Hoogsteen (G: C or A: A: T) hydrogen bonds. (Taken from Chan et al, 2011)

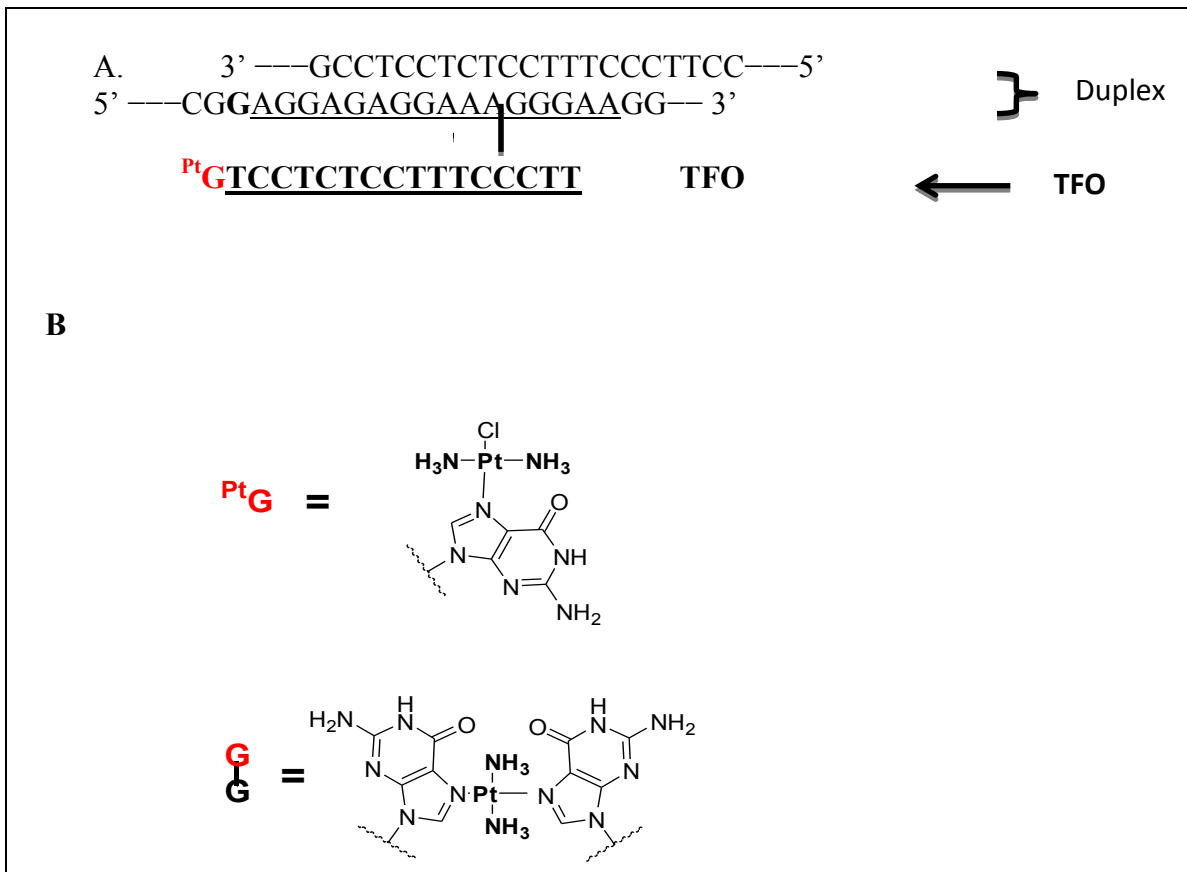
Figure 1:



**Figure 2: Schematic representation of TFO cross-linking to its target DNA duplex.**

(A) TFO is platinated on the N7 of guanine and the platinated TFO forms an adduct with a adjacent guanine in the DNA target. (B) A representation the TFO –DNA adduct formation. (Taken from Miller, 2011-Lecture notes).

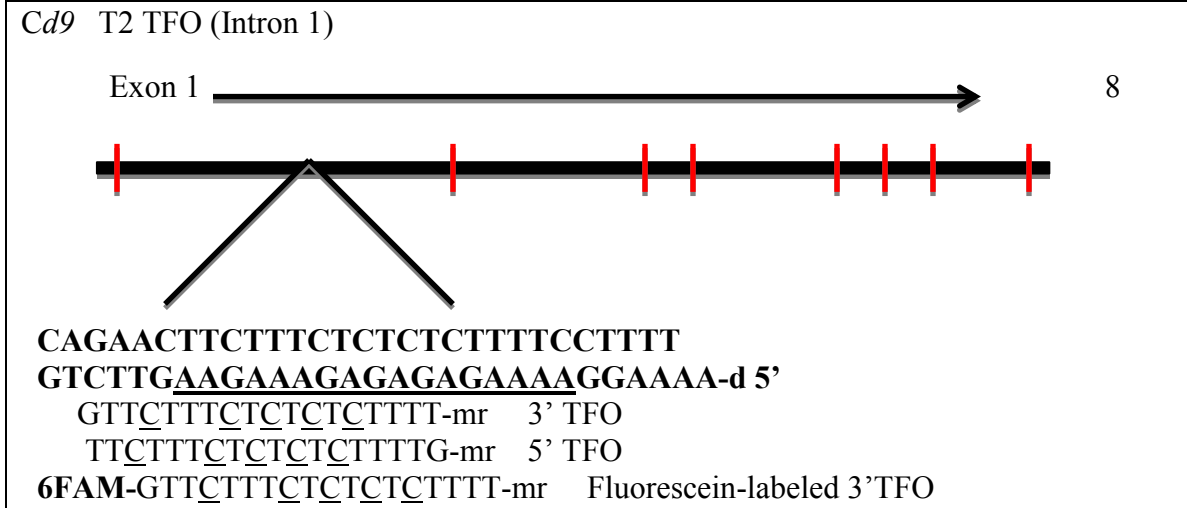
Figure 2:



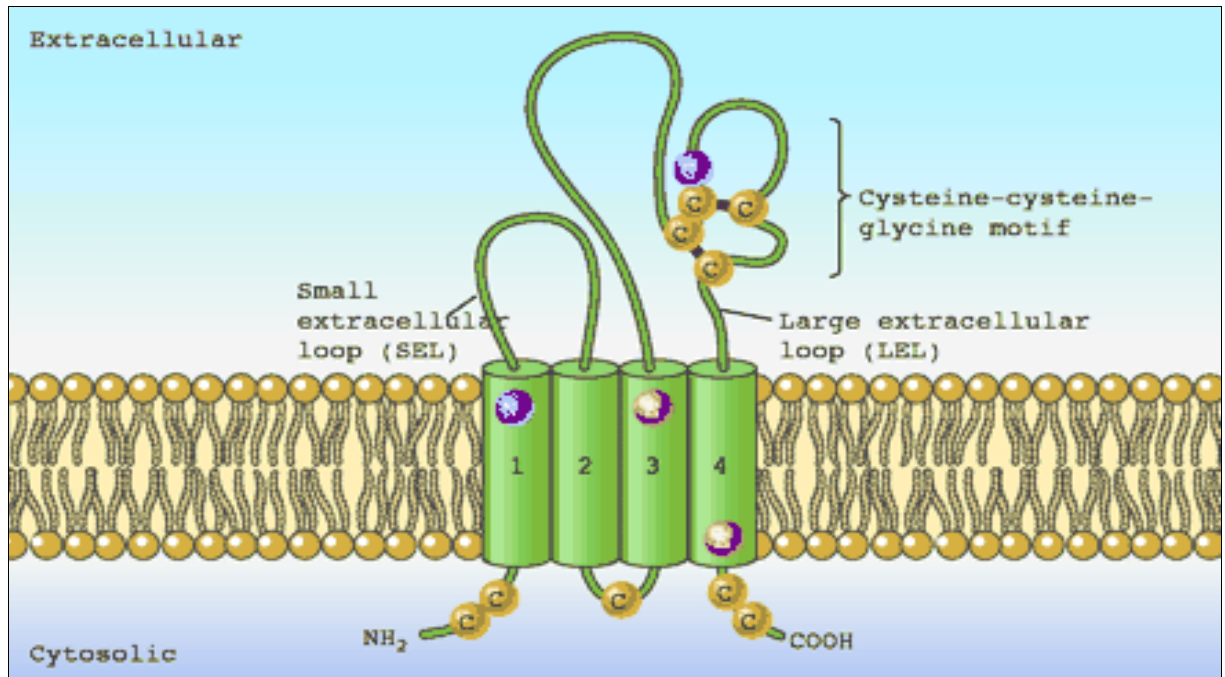
**Figure 3: Schematic representation of the *Cd9* target and the structural features of CD9 protein.** (A) Schematic representation of the *Cd9* T2 target. (B) The general structure of Tetraspanins membrane proteins. Tetraspanins are composed of 4 transmembrane domains with two extracellular loops, which mediate protein-protein interactions and a cytoplasmic region involved in signaling (Taken from Levy and Shosham, 2005).

Figure 3:

A.



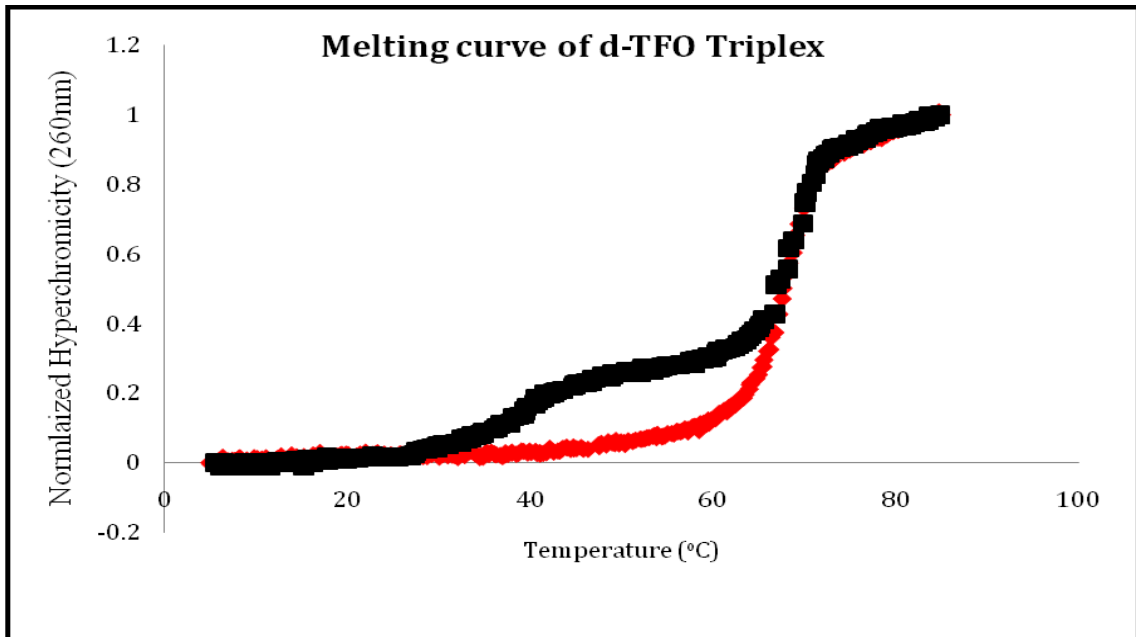
B.



**Figure 4: General representation of the thermal denaturation curve and the melting temperatures of all deoxyribonucleotides TFO. (A)** A general representation of thermal denaturation of deoxyribose triplexes. Binding stability of the d-TFO with the DNA duplex is examined by thermal denaturation experiments. The DNA duplex (0.5  $\mu$ M) is incubated with 0.5  $\mu$ M d-TFO in pH 7 triplex buffer [50 mM 2-(N -morpholino) ethanesulfonic acid or 50 mM 3-(N -morpholino) propanesulfonic acid, 100 mM NaCl, and 5 mM  $MgCl_2$  ] at 90°C for 10mins and cooled to room temperature. The absorbance of the reaction mixture was determined using a UV-Spectrophotometer. The normalized hyperchromicity  $(A_0-A_1)/(A_f-A_1)$  is plotted against temperature to determine the melting temperature of the triplex. d-deoxyribonucleotide TFO, A-absorbance. The triplex is represented by the black curve and the DNA duplex is represented by the red curve. **(B)** Melting temperatures of the third strand of the triplex formed by deoxyribose TFOs.



**Figure 4:**



**A**

**B**

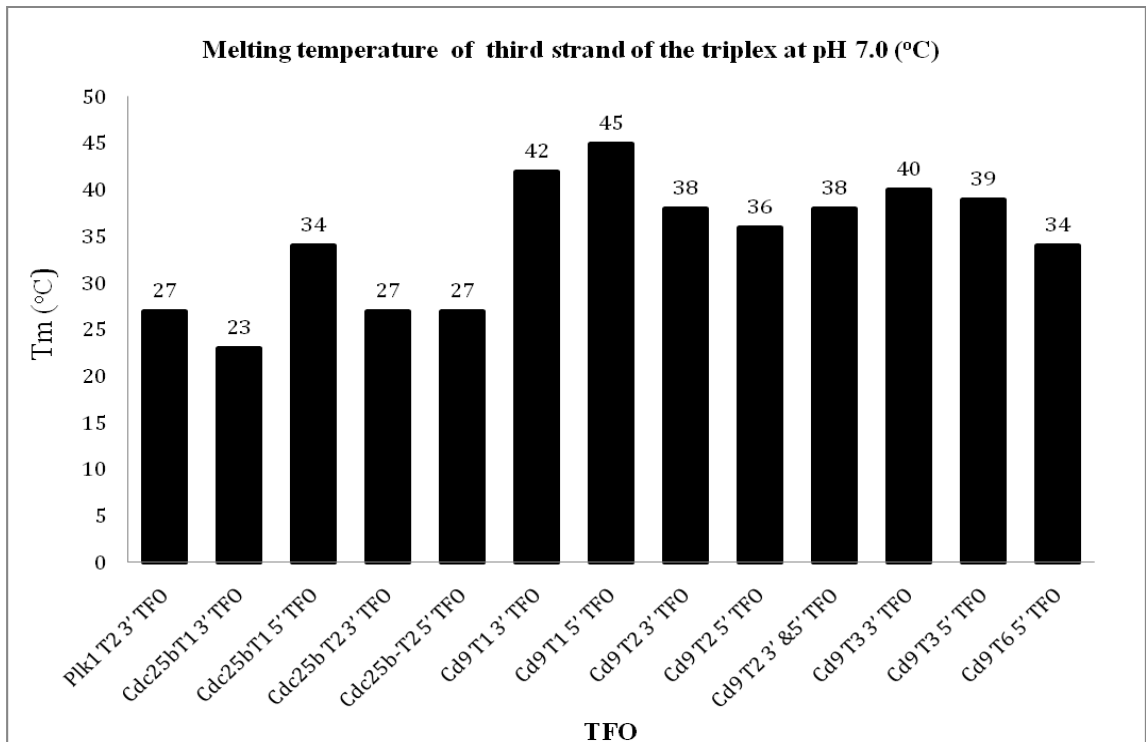


**Figure 5: Cross-linking reaction of d-TFO with DNA duplex. (A)** General representation of cross-linking reaction of Pt-TFO with DNA duplex. A 1  $\mu\text{M}$  solution of  $^{32}\text{P}$  labeled DNA was incubated with 0, 1, 5 and 10  $\mu\text{M}$  in triplex buffer [50 mM 2-(N-morpholino) ethanesulfonic acid or 50 mM 3-(N-morpholino) propanesulfonic acid, 100 mM NaCl, and 5 mM  $\text{MgCl}_2$ ] for 18 h at 37°C and the resulting reaction mixtures were analyzed by electrophoresis on 20% denaturing polyacrylamide gel. The dotted arrow indicates the position of the triplex and the solid arrow indicates the position of the DNA duplex. **(B)** Pt-TFO (10  $\mu\text{M}$ ) was incubated with 1  $\mu\text{M}$  of DNA duplex in pH 6.0 and pH 7.0 triplex buffer [50 mM 2-(N-morpholino) ethanesulfonic acid or 50 mM 3-(N-morpholino) propanesulfonic acid, 100 mM NaCl, and 5 mM  $\text{MgCl}_2$ ] and percent cross-linking of each Pt-TFO was determined by phosphoimaging. The percent cross-linking was graphed against the corresponding Pt-TFO.

**Figure 5:**

**A**

[Pt-TFO]  $\mu$ M

0      1      5      10



**B**

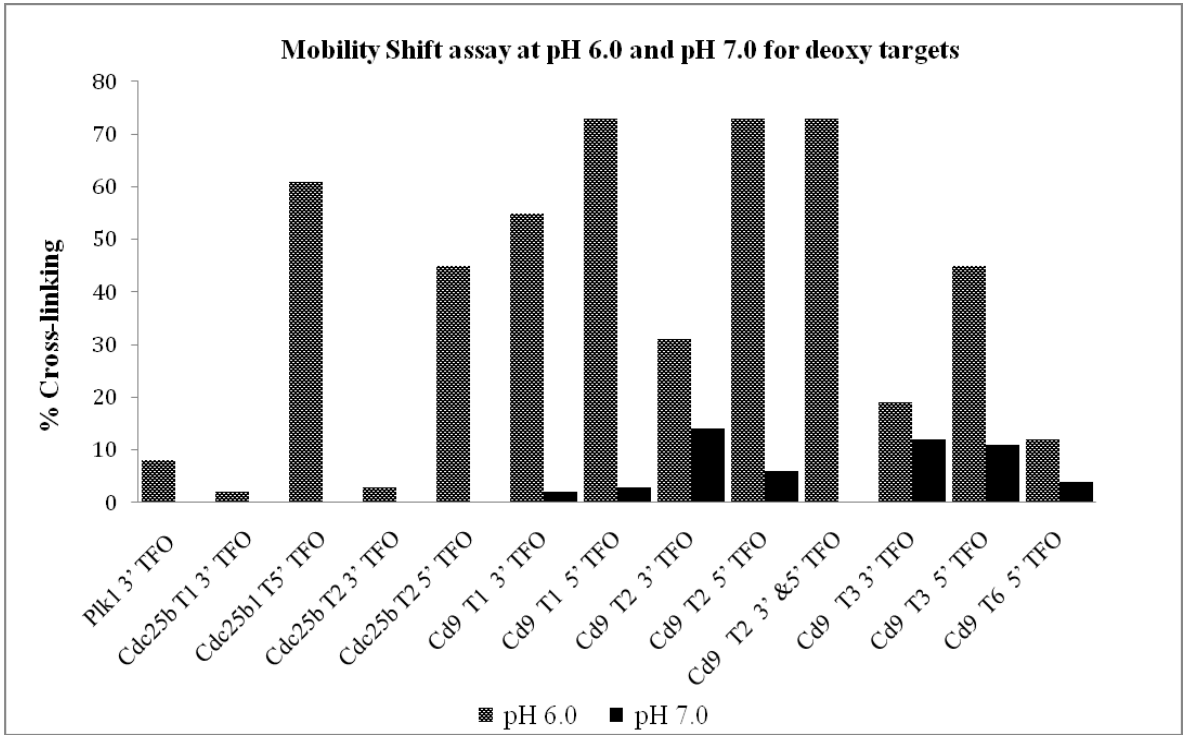


**Figure 6. General thermal denaturation curve of 2' 0-methylribonucleotide triplex.**

The DNA duplex (0.5  $\mu\text{M}$ ) is incubated with 0.5  $\mu\text{M}$  *Cd9* specific TFO, Pt-*Cd9* specific TFO, Scrambled TFO or Pt-Scrambled TFO in pH 7 triplex buffer [50 mM 2-(N -morpholino) ethanesulfonic acid or 50 mM 3-(N -morpholino) propanesulfonic acid, 100 mM NaCl, and 5 mM  $\text{MgCl}_2$ ] at 90°C for 10 mins and cooled to room temperature and the absorbance of the reaction mixture determined by a UV-Spectrophotometer with gradual increments in temperature (4°C to 85°C). The normalized hyperchromicity ( $A_{0-A1}/(A_f-A1)$ ) is plotted against temperature to determine the melting temperature of the triplex. The black curve denotes the duplex, red curve denotes the TFO.

**Figure 6:**

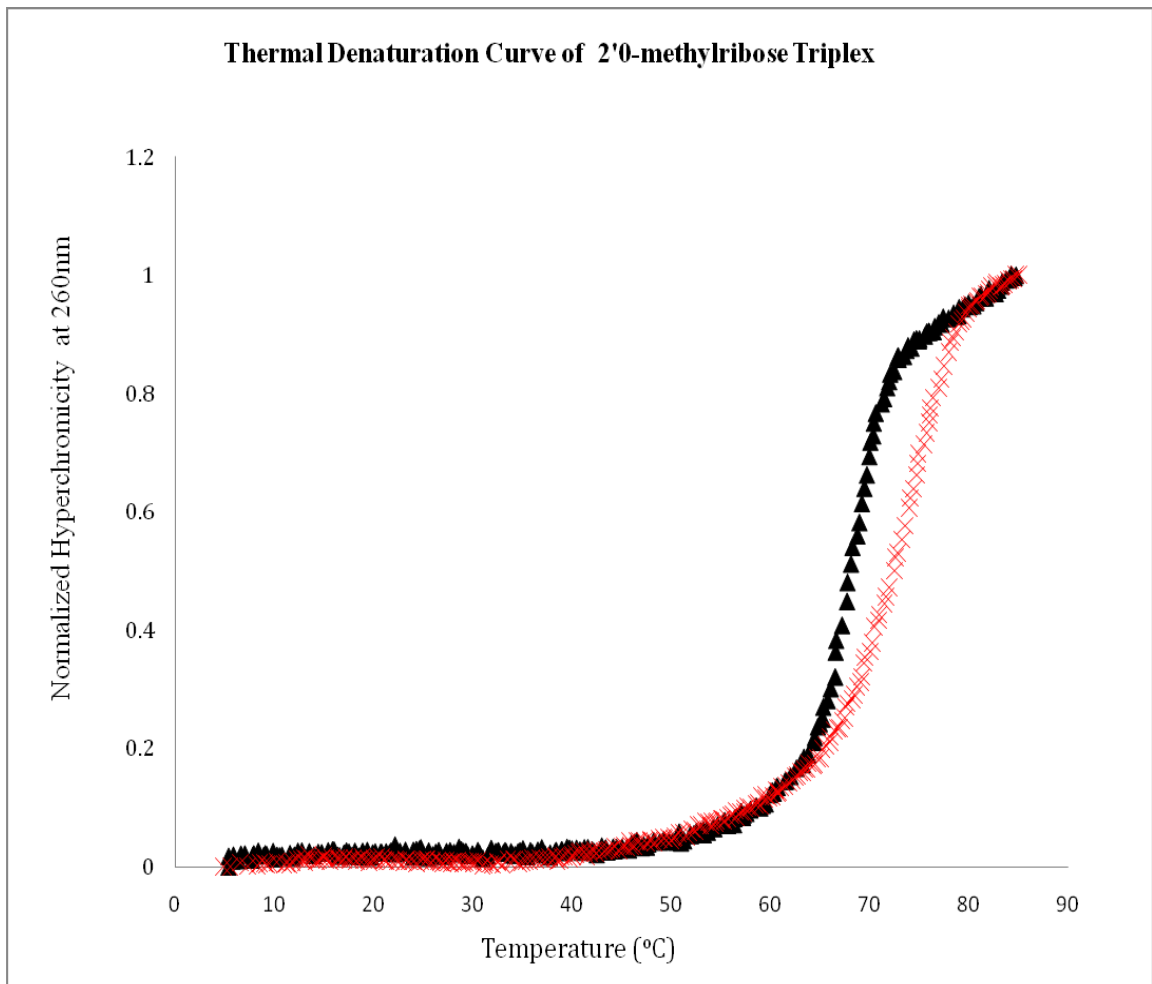
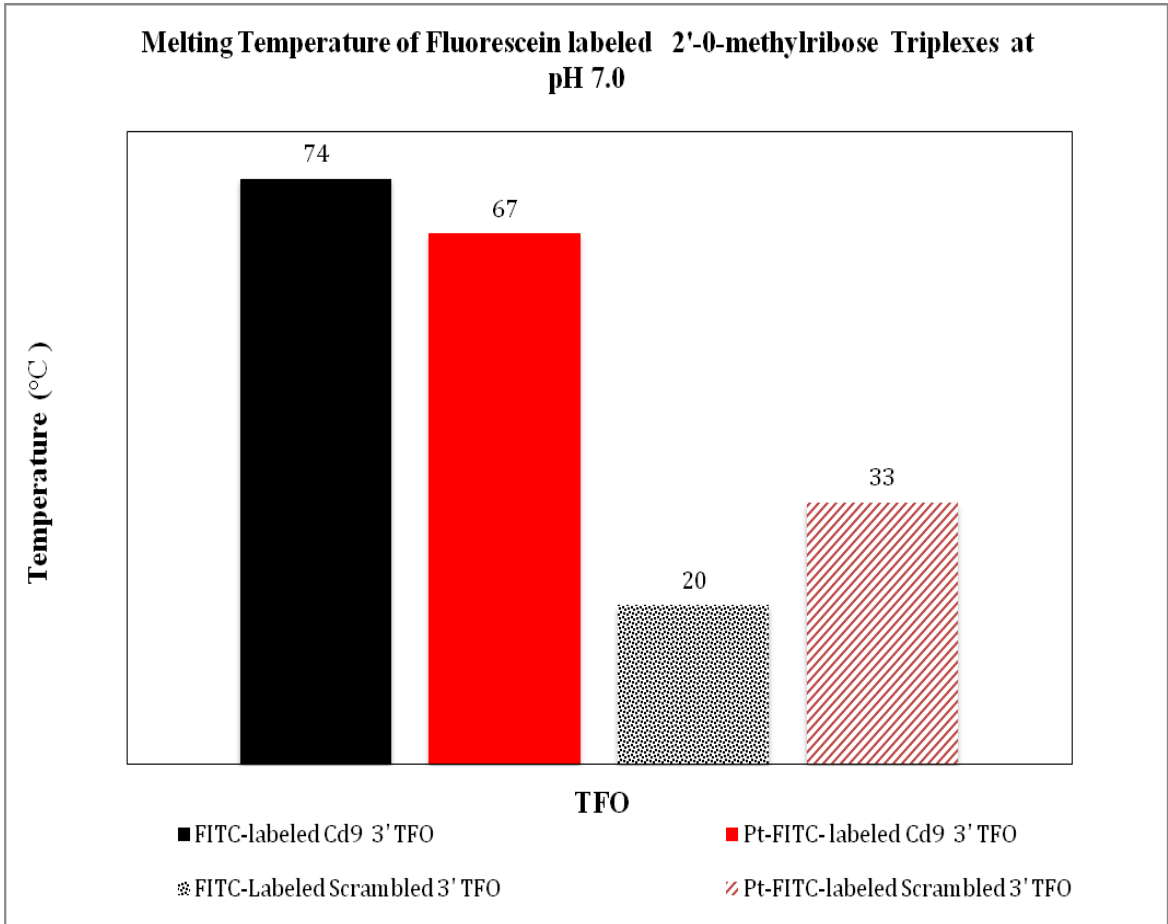


**Figure 7. Melting temperature and electrophoretic mobility shift assay (cross-linking) of 2'-0-methyl *Cd9* T2 3' *Cd9* T2 3' TFO and FITC-labeled *Cd9* T2 3' and Scrambled 3' TFO.** (A) Melting temperatures of the third strand of the triplex formed by of 2'-0-methyl *Cd9* T2 3' *Cd9* T2 3' TFO and fluorescein labeled *Cd9* T2 3' and Scrambled 3' TFO in pH 7.0 triplex buffers. (B) Cross-linking between platinated 2' 0-methylribonucleotides *Cd9* 3' TFO and FITC-labeled *Cd9* 3' TFO or Scrambled TFO and their respective DNA duplexes. Solutions containing 10  $\mu$ M of Pt- *Cd9* T2 3' TFO, Pt-FITC *Cd9* T2 3' TFO and Pt-FITC labeled Scrambled 3' TFO and the 1  $\mu$ M  $^{32}$ P-labeled DNA duplex were incubated in pH 6, pH 7, pH 7.5 triplex buffers for 18 h at 37°C and the reaction mixtures were analyzed by electrophoresis on denaturing 20% polyacrylamide gel. Percent cross-linking of Pt-TFO were determined by phosphoimaging. The dashed arrow denotes the triplex and the solid arrow denotes the duplex. **Key:** D=duplex, SC=FITC-labeled Pt-Scrambled 3' TFO, *Cd9* 1 =Pt-*Cd9* T2 3' TFO, *Cd9* 2 = FITC-labeled Pt *Cd9* 3'TFO

**Figure 7:**

**A**



**B**

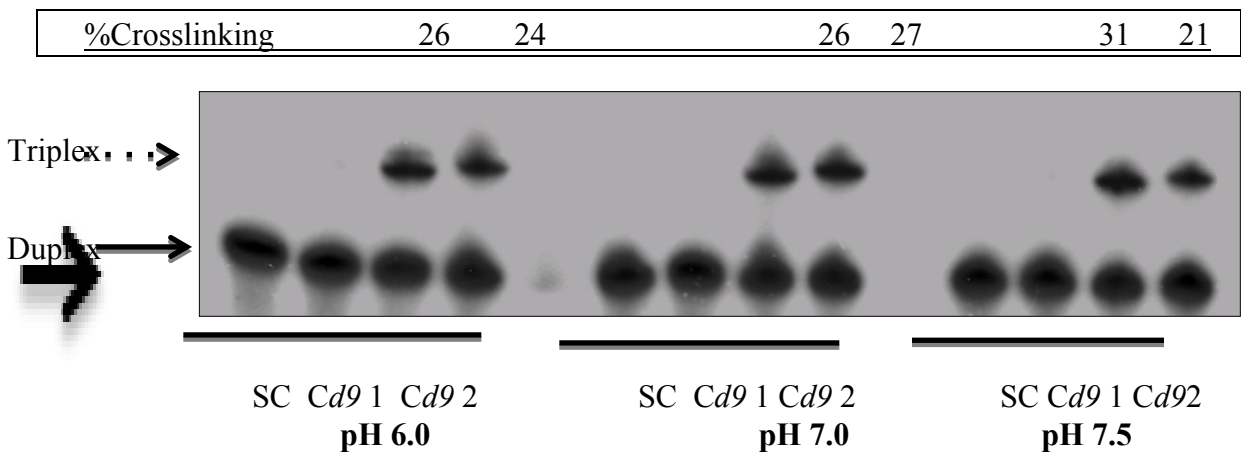
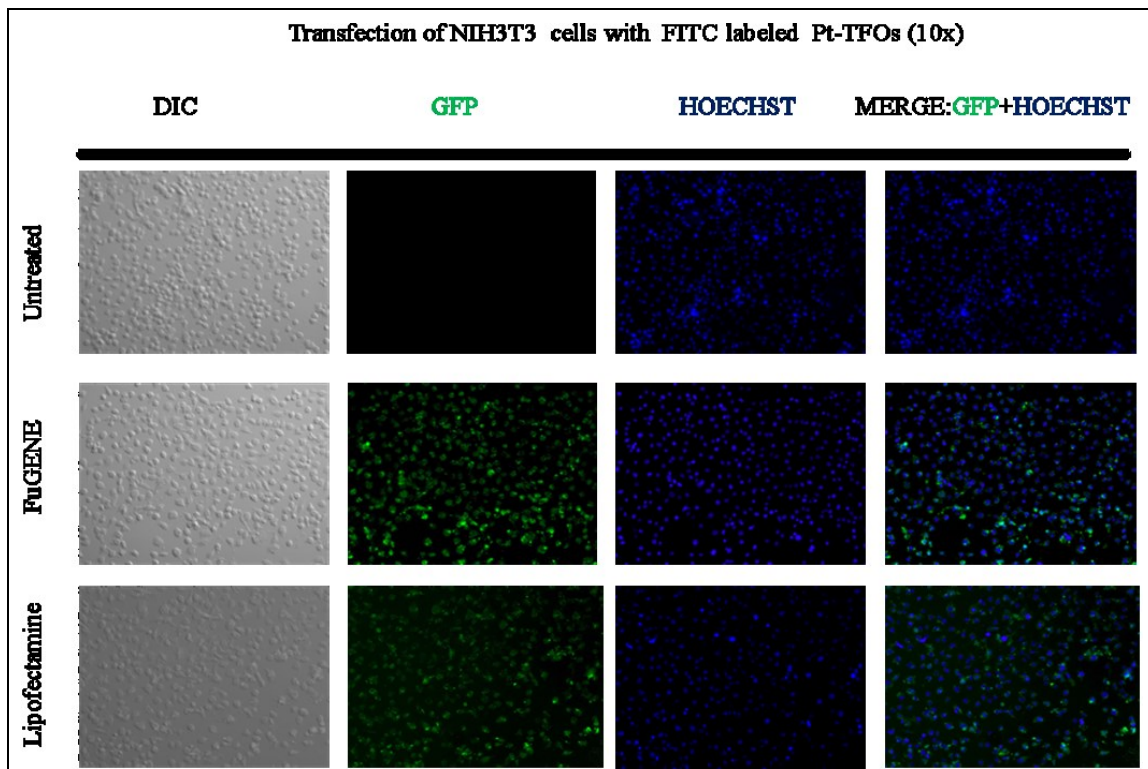


**Figure 8. Transfection of NIH3T3 cells with FITC-labeled inert Pt-Cd9 specific 3' TFO. (A)** NIH3T3 cells were transfected with FITC-labeled inert Pt-TFO using either FuGENE HD (panel 2) or Lipofectamine 2000 (panel 3) transfection reagents in a 1:3 TFO to transfection reagent ratio and incubated for 72 hours and 48 hours respectively. The cells were stained with Hoechst (blue-DNA) and analyzed by live cell fluorescence microscopy (10x). Uptake efficiency determined by counting total number of TFO per DNA per image. Three images were taken and averaged. **(B)** Higher magnification (40X) live cell imaging of FITC-labeled Inert-TFO images of transfected cells to determine localization of the inert Pt-TFO.

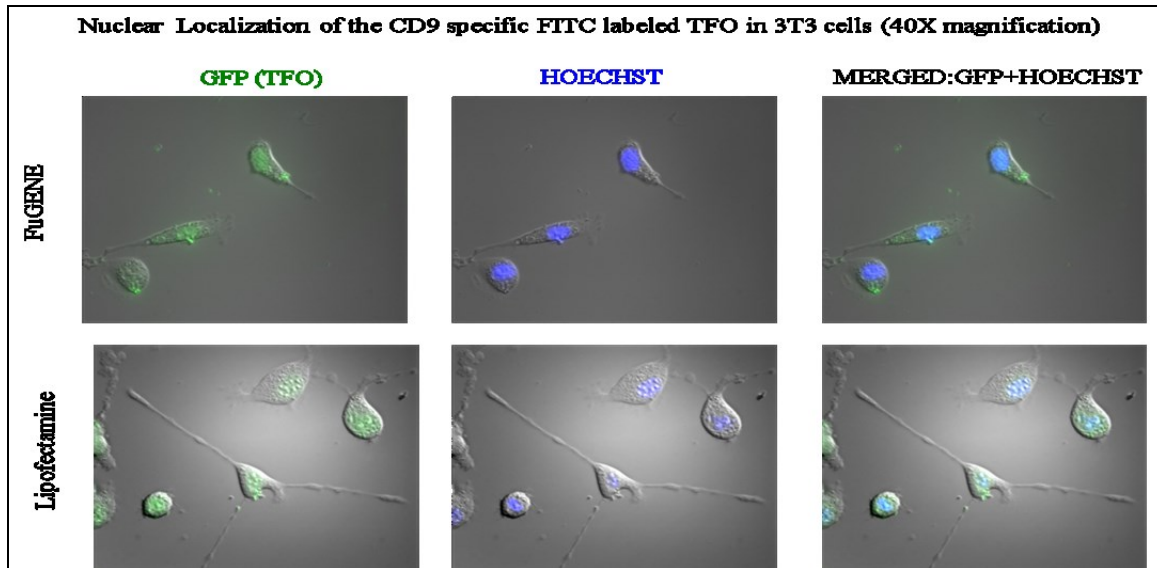


Figure 8:

A.



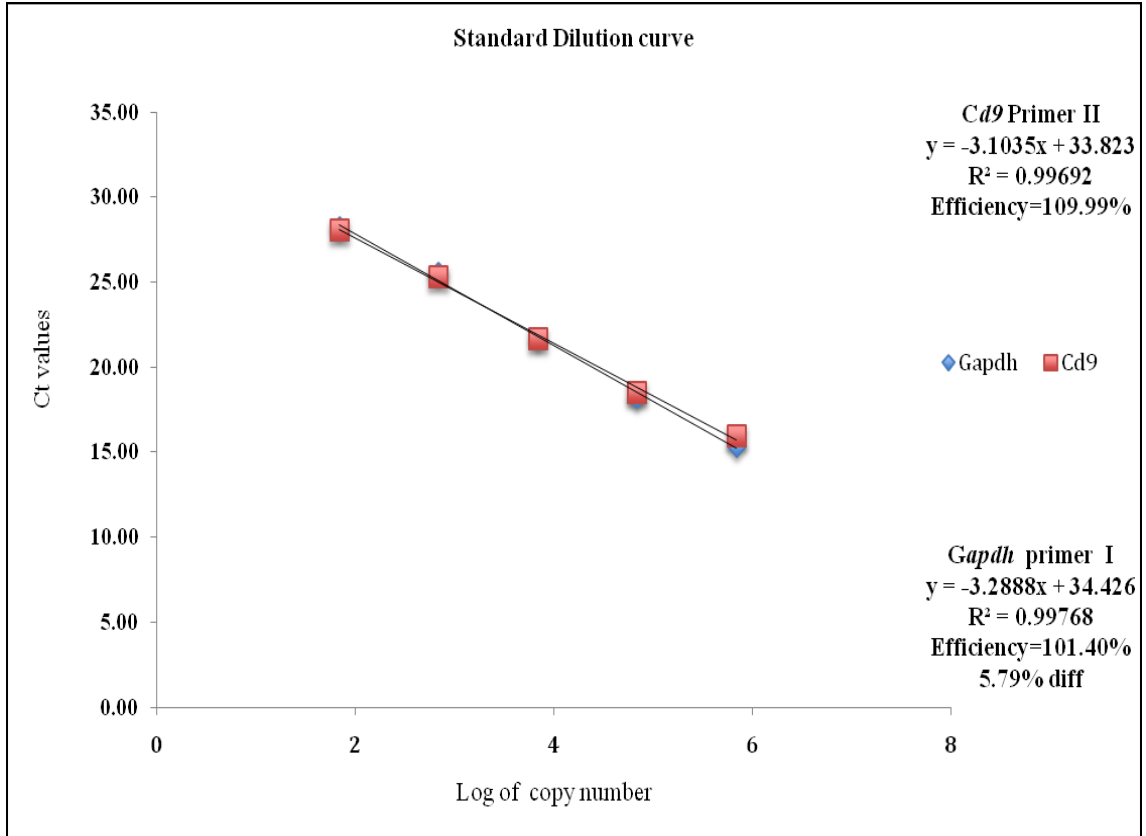
B.



**Figure 9: RT-qPCR optimization - Standard curve and agarose gel.** (A) Standard curve obtained from 10-fold dilutions of cDNA reversed transcribed from RNA extracted from NIH3T3 Cells incubated for 72 hours. Ct values are obtained as an average of a triplicate. The blue line is the *Gapdh* primer and the red line is the *Cd9* primer. (B) The RT-qPCR product run on 1.5% agarose gel pre-stained with SYBR green to confirm the primer products. Lane 1 and 4 is 10 uL of 1.5 uL of 10 ng/uL LMW marker in 9 uL of loading buffer. Lane 2 is 10 uL of 3 uL of *Cd9* qPCR product in 8 uL of loading buffer. Lane 3 is 10 uL of 3 uL of *Gapdh* qPCR product in 8 uL of loading buffer.

**Figure 9:**

**A**



**B**

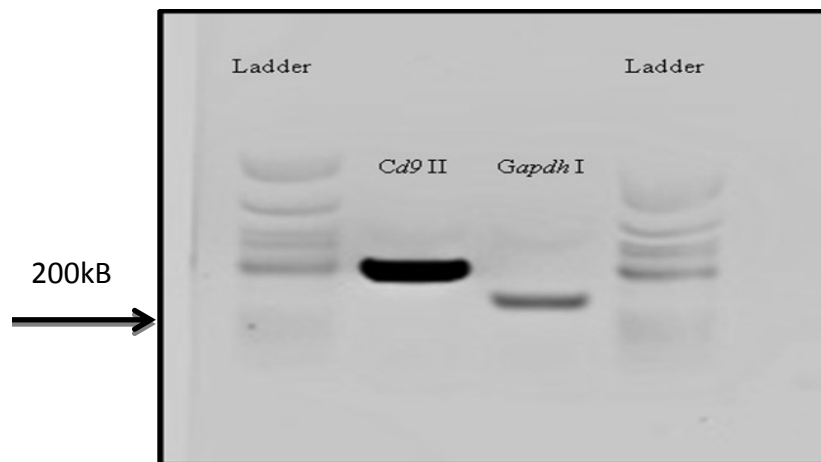


**Figure 10: Quantitative evaluation of *Cd9*mRNA expression in NIH3T3 determined by RT-qPCR post transfection with *Cd9* T2 TFO.** Data represents the change in mRNA transcript levels as measured by RT-qPCR. Relative mRNA expression levels for *Cd9* in untreated, FITC-labeled Pt- Pt-scrambled TFO and FITC-labeled Pt- *Cd9* T2 3' TFO transfected cells using either FuGENE HD or Lipofectamine 2000 as quantified by RT-qPCR. The relative expressions were determined using the  $2^{\Delta\Delta Ct}$  methods with *Gapdh* as the endogenous control. Data represents the mean of two independent experiments, each performed in triplicate +/- standard deviation.

**Figure 10**

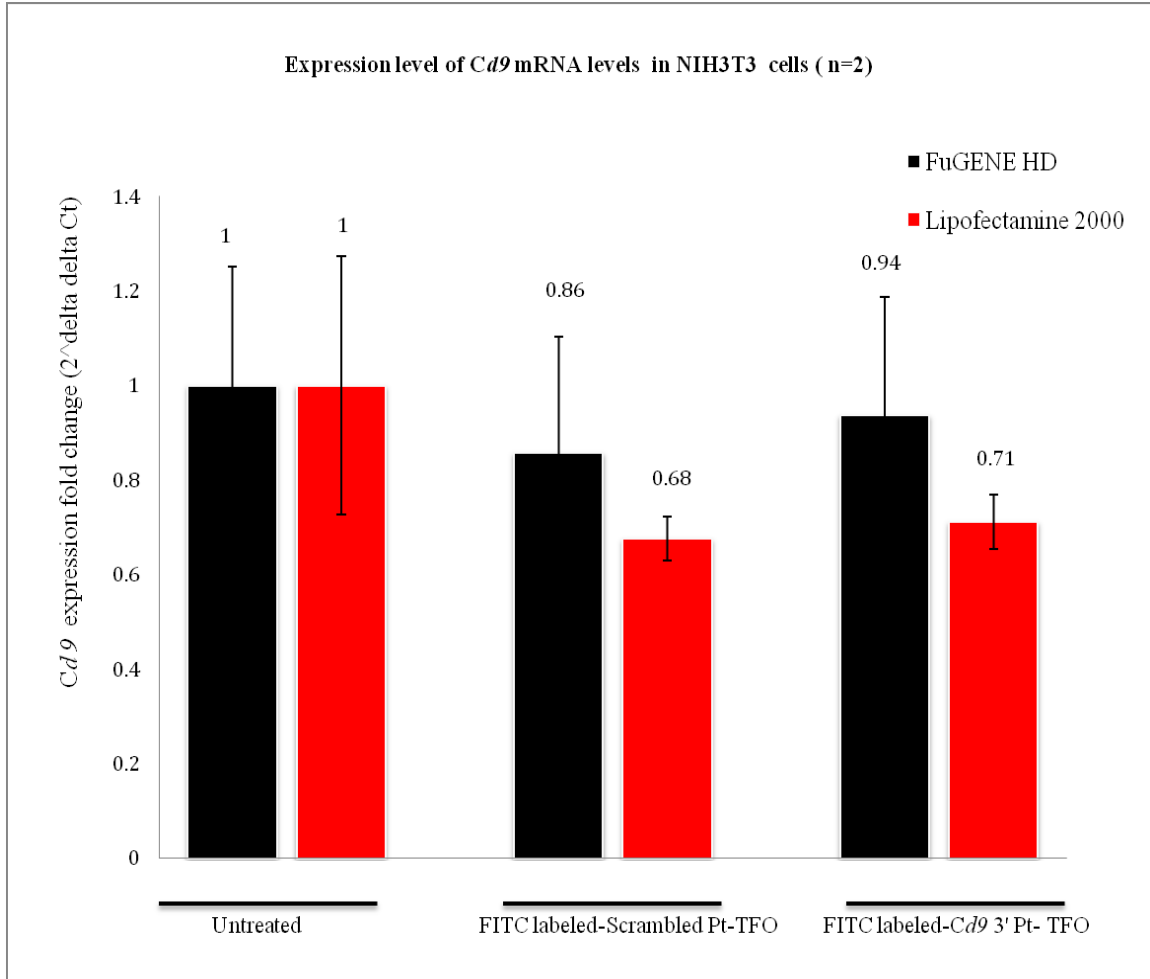
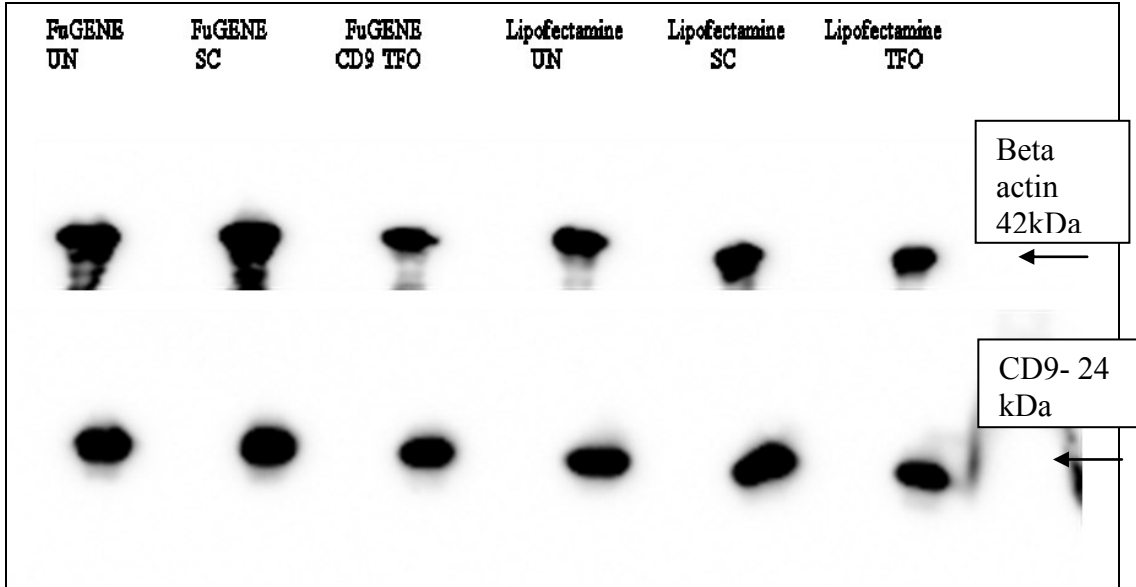


**Figure 11: Quantitative evaluation of inhibition of the CD9 protein in NIH3T3**

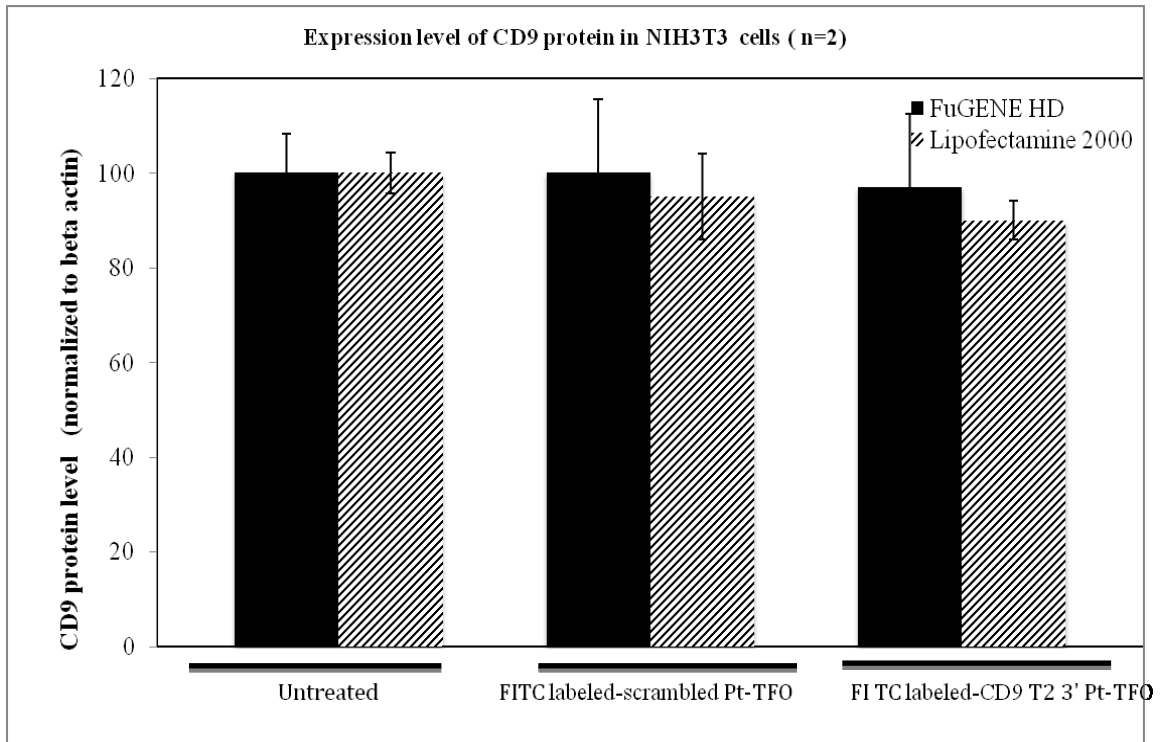
**evaluated by Western blotting.** NIH3T3 cells were transfected with only the transfection reagent (Lipofectamine™ 2000 and FuGENE HD), FITC-labeled Scrambled 3' TFO, or FITC-labeled CD9 T2 3' TFO. NIH3T3 lysates collected after treatment with TFO and probed with the CD9 antibody (lower panel) and top blot probed with the beta-actin antibody (upper panel). The band intensities of the CD9 proteins were normalized to the beta actin and compared to the untreated control. Data represent means of two replicates  $\pm$  standard deviation. Transfection of FITC-labeled CD9 T2 3' TFO in mouse NIH3T3 using either FuGENE HD or Lipofectamine does not change the protein expression of the CD9 TFO.

Figure 11

A



B



## References

- Adolf, M. S., Aschberger, T., & Pelster, B. (2013). *A method to evaluate the efficiency of transfection reagents in an adherent zebrafish cell line*  
doi:10.1089/biores.2012.0287
- Arnold, D. R., Françon, P., Zhang, J., Martin, K., & Clarke, H. J. (2008). Stem-loop binding protein expressed in growing oocytes is required for accumulation of mRNAs encoding histones H3 and H4 and for early embryonic development in the mouse. *Developmental Biology*, 313(1), 347-358.
- Austin, C. P., Battey, J. F., Bradley, A., Bucan, M., Capecchi, M., Collins, F. S., . . . Nagy, A. (2004). The knockout mouse project. *Nature Genetics*, 36(9), 921-924.  
doi:10.1038/ng0904-921
- Barton, G. M., & Medzhitov, R. (2002). Retroviral delivery of small interfering RNA into primary cells. *Proceedings of the National Academy of Sciences*, 99(23), 14943-14945. doi:10.1073/pnas.242594499
- Basye, J., Trent, J. O., Gao, D., & Ebbinghaus, S. W. (2001). Triplex formation by morpholino oligodeoxyribonucleotides in the HER-2/neu promoter requires the pyrimidine motif. *Nucleic Acids Research*, 29(23), 4873-4880.  
doi:10.1093/nar/29.23.4873



- Berditchevski, F., & Odintsova, E. (1999). Characterization of Integrin–Tetraspanin adhesion complexes: Role of tetraspanins in integrin signaling. *The Journal of Cell Biology*, *146*(2), 477-492. doi:10.1083/jcb.146.2.477
- Boucheix, C., & Rubinstein, E. (2001). Tetraspanins. *Cellular and Molecular Life Sciences CMLS*, *58*(9), 1189-1205. doi:10.1007/PL00000933
- Campbell, M. A., & Miller, P. S. (2009a). Cross-linking to an interrupted polypurine sequence with a platinum-modified triplex-forming oligonucleotide. *Journal of Biological Inorganic Chemistry*, *14*(6), 873-881. doi:10.1007/s00775-009-0499-3
- Campbell, M. A., & Miller, P. S. (2009b). Transplatin-conjugated triplex-forming oligonucleotides form adducts with both strands of DNA. *Bioconjugate Chemistry*, *20*(12), 2222-2230. doi:10.1021/bc900008s
- Chan, P. P., & Glazer, P. M. (1997). Triplex DNA: Fundamentals, advances, and potential applications for gene therapy. *Journal of Molecular Medicine*, *75*(4), 267-282. doi:10.1007/s001090050112
- Chen, H., & Sampson, N. S. (1999). Mediation of sperm-egg fusion: Evidence that mouse egg  $\alpha 6 \beta 1$  integrin is the receptor for sperm fertilin<sup>2</sup> [Abstract]. *Chemistry & Biology*, *6*(1) 1-10.
- Colombier, C., Lippert, B., & Leng, M. (1996). Interstrand cross-linking reaction in triplexes containing a monofunctional transplatin-adduct. *Nucleic Acids Research*, *24*(22), 4519-4524. doi:10.1093/nar/24.22.4519

- Cooney, M., Czernuszewicz, G., Postel, E., Flint, S., & Hogan, M. (1988). Site-specific oligonucleotide binding represses transcription of the human c-myc gene in vitro. *Science*, *241*(4864), 456-459. doi:10.1126/science.3293213
- Crooke, S. T. (1992). Therapeutic applications of oligonucleotides. *Nat Biotech*, *10*(8), 882-886.
- Dassie, J. P., Liu, X., Thomas, G. S., Whitaker, R. M., Thiel, K. W., Stockdale, K. R., . . . Giangrande, P. H. (2009). Systemic administration of optimized aptamer-siRNA chimeras promotes regression of PSMA-expressing tumors. *Nat Biotech*, *27*(9), 839-846.
- Dias, N., & Stein, C. A. (2002). Antisense oligonucleotides: Basic concepts and mechanisms. *Molecular Cancer Therapeutics*, *1*(5), 347-355.
- Draetta, G., & Eckstein, J. (1997). Cdc25 protein phosphatases in cell proliferation. *Biochimica Et Biophysica Acta (BBA) - Reviews on Cancer*, *1332*(2), M53-M63. doi:10.1016/S0304-419X(96)00049-2
- Duan, Y., Zhang, S., Wang, B., Yang, B., & Zhi, D. (2009). The biological routes of gene delivery mediated by lipid-based non-viral vectors. *Expert Opinion on Drug Delivery*, *6*(12), 1351-1361. doi:10.1517/17425240903287153
- Duval-Valentin, G., Thuong, N. T., & Helene, C. (1992). Specific inhibition of transcription by triple helix-forming oligonucleotides. *Proceedings of the National Academy of Sciences of the United States of America*, *89*(2), 504-508.

- Eckerdt, F., Yuan, J., & Strebhardt, K. (2005). Polo-like kinases and oncogenesis. *Oncogene*, 24(2), 267-276. doi:10.1038/sj.onc.1208273
- Escudé, C., Sun, J. S., Rougée, M., Garestier, T., & Hélène, C. (1992). Stable triple helices are formed upon binding of RNA oligonucleotides and their 2'-O-methyl derivatives to double-helical DNA. *C R Acad Sci III*, 315(13), 521-525.
- Escudé, C., François, J., Sun, J., Ott, G., Sprinzl, M., Garestier, T., & Héle`ne, J. (1993). Stability of triple helices containing RNA and DNA strands: Experimental and molecular modeling studies. *Nucleic Acids Research*, 21(24), 5547-5553. doi:10.1093/nar/21.24.5547
- Faria, M., Wood, C. D., Perrouault, L., Nelson, J. S., Winter, A., White, M. R. H., . . . Giovannangeli, C. (2000). Targeted inhibition of transcription elongation in cells mediated by triplex-forming oligonucleotides. *Proceedings of the National Academy of Sciences*, 97(8), 3862-3867. doi:10.1073/pnas.97.8.3862
- Faruqi, A. F., Seidman, M. M., Segal, D. J., Carroll, D., & Glazer, P. M. (1996). Recombination induced by triple-helix-targeted DNA damage in mammalian cells. *Molecular and Cellular Biology*, 16(12), 6820-6828.
- Faruqi, A. F., Datta, H. J., Carroll, D., Seidman, M. M., & Glazer, P. M. (2000). Triple-helix formation induces recombination in mammalian cells via a nucleotide excision repair-dependent pathway. *Molecular and Cellular Biology*, 20(3), 990-1000. doi:10.1128/MCB.20.3.990-1000.2000

FAU, D. J., FAU, L. X., FAU, T. G., FAU, W. R., FAU, T. K., FAU, S. K., . . .

Giangrande, P. H. (1229). *Systemic administration of optimized aptamer-siRNA chimeras promotes regression of PSMA-expressing tumors*

Fedoriw, A. M., Stein, P., Svoboda, P., Schultz, R. M., & Bartolomei, M. S. (2004).

Transgenic RNAi reveals essential function for CTCF in H19 gene imprinting.

*Science*, 303(5655), 238-240.

Felgner, P. L., Gadek, T. R., Holm, M., Roman, R., Chan, H. W., Wenz, M., . . .

Danielsen, M. (1987). Lipofection: A highly efficient, lipid-mediated DNA-

transfection procedure. *Proceedings of the National Academy of Sciences*, 84(21),

7413-7417.

Felgner, P. L., & Ringold, G. M. (1989). Cationic liposome-mediated transfection.

*Nature*, 337(6205), 387-388.

Felsenfeld, G., & Rich, A. (1957). Studies on the formation of two- and three-stranded

polyribonucleotides. *Biochimica Et Biophysica Acta*, 26(3), 457-468.

doi:10.1016/0006-3002(57)90091-4

Fox, K. R. (2000). Targeting DNA with triplexes. *Current Medicinal Chemistry*, 7(1), 17-

37. doi:<http://dx.doi.org.proxy1.library.jhu.edu/10.2174/0929867003375506>

Frank-Kamenetskii, M., & Mirkin, S. M. (1995). Triplex DNA structures. *Annual Review*

*of Biochemistry*, 64(1), 65-95. doi:10.1146/annurev.bi.64.070195.000433

- Gaddis, S. S., Wu, Q., Thames, H. D., Digiovanni, J., Walborg, E. F., Macleod, M. C., & Vasquez, K. M. (2006). A web-based search engine for triplex-forming oligonucleotide target sequences. *Oligonucleotides*, *16*(2), 196-201.
- Galaktionov, K., & Beach, D. (1991). Specific activation of cdc25 tyrosine phosphatases by B-type cyclins: Evidence for multiple roles of mitotic cyclins [Abstract]. *Cell*, *67*(6) 1181-1194.
- Gershon, E., Galiani, D., & Dekel, N. (2006). Cytoplasmic polyadenylation controls cdc25B mRNA translation in rat oocytes resuming meiosis. *Reproduction*, *132*(1), 21-31. doi:10.1530/rep.1.01093
- Glare, E. M., Divjak, M., Bailey, M. J., & Walters, E. H. (2002).  $\beta$ -actin and GAPDH housekeeping gene expression in asthmatic airways is variable and not suitable for normalising mRNA levels. *Thorax*, *57*(9), 765-770. doi:10.1136/thorax.57.9.765
- Glazar, A. I., & Evans, J. P. (2009). Immunoglobulin superfamily member IgSF8 (EWI-2) and CD9 in fertilisation: Evidence of distinct functions for CD9 and a CD9-associated protein in mammalian sperm-egg interaction. *Reproduction, Fertility and Development*, *21*(2), 293-303.
- Glover, D. M., Hagan, I. M., & Tavares, Á A. M. (1998). Polo-like kinases: A team that plays throughout mitosis. *Genes & Development*, *12*(24), 3777-3787. doi:10.1101/gad.12.24.3777

- Gorzelniaak, K., Janke, J., Engeli, S., & Sharma, A. M. (2001). Validation of endogenous controls for gene expression studies in human adipocytes and preadipocytes. *Horm Metab Res*, 33(10), 625-627.
- Graham, M., & Miller, P. (2012). Inhibition of transcription by platinated triplex-forming oligonucleotides. *JBIC Journal of Biological Inorganic Chemistry*, 17(8), 1197-1208. doi:10.1007/s00775-012-0933-9
- Guieysse, A., Praseuth, D., Giovannangeli, C., Asseline, U., & Hélène, C. (2000). Psoralen adducts induced by triplex-forming oligonucleotides are refractory to repair in HeLa cells. *Journal of Molecular Biology*, 296(2), 373-383. doi:10.1006/jmbi.1999.3466
- Han, S. J., Chen, R., Paronetto, M. P., & Conti, M. (2005). *Curr.Biol*, 15, 1670-1676.
- Havre, P. A., Gunther, E. J., Gasparro, F. P., & Glazer, P. M. (1993). Targeted mutagenesis of DNA using triple helix-forming oligonucleotides linked to psoralen. *Proceedings of the National Academy of Sciences of the United States of America*, 90(16), 7879-7883.
- Hemler, M. E. (2001). Specific tetraspanin functions. *The Journal of Cell Biology*, 155(7), 1103-1108. doi:10.1083/jcb.200108061
- Hemler, M. E. (2003). TETRASPANIN PROTEINS MEDIATE CELLULAR PENETRATION, INVASION, AND FUSION EVENTS AND DEFINE A NOVEL TYPE OF MEMBRANE MICRODOMAIN. *Annual Review of Cell and*

*Developmental Biology*, 19(1), 397-422.

doi:10.1146/annurev.cellbio.19.111301.153609

Huang, H., Chen, P., Yu, C., Chuang, C., Stone, L., Hsiao, W., . . . Kuo, H. (2011).

Epithelial cell adhesion molecule (EpcAM) complex proteins promote transcription factor-mediated pluripotency reprogramming. *Journal of Biological Chemistry*,

286(38), 33520-33532. doi:10.1074/jbc.M111.256164

Igarashi, H., Knott, J. G., Schultz, R. M., & Williams, C. J. (2007). Alterations of PLCβ1 in mouse eggs change calcium oscillatory behavior following fertilization.

*Developmental Biology*, 312(1), 321-330.

Inoue, H., Hayase, Y., Imura, A., Iwai, S., Miura, K., & Ohtsuka, E. (1987). Synthesis

and hybridization studies on two complementary nona(2'-O-methyl)ribonucleotides.

*Nucleic Acids Research*, 15(15), 6131-6148. doi:10.1093/nar/15.15.6131

Ito, J., Yoon, S., Lee, B., Vanderheyden, V., Vermassen, E., Wojcikiewicz, R., . . .

Fissore, R. A. (2008). Inositol 1,4,5-trisphosphate receptor 1, a widespread Ca<sup>2+</sup> channel, is a novel substrate of polo-like kinase 1 in eggs. *Developmental Biology*,

320(2), 402-413. doi:10.1016/j.ydbio.2008.05.548

Kaji, K., Oda, S., Miyazaki, S., & Kudo, A. (2002). Infertility of CD9-deficient mouse

eggs is reversed by mouse CD9, human CD9, or mouse CD81; polyadenylated mRNA injection developed for molecular analysis of Sperm–Egg fusion.

*Developmental Biology*, 247(2), 327-334. doi:10.1006/dbio.2002.0694

- Kaji, K., Oda, S., Shikano, T., Ohnuki, T., Uematsu, Y., Sakagami, J., . . . Kudo, A. (2000). The gamete fusion process is defective in eggs of Cd9-deficient mice. *Nature Genetics*, 24(3), 279.
- Kibbe, W. A. (2007). *OligoCalc: An online oligonucleotide properties calculator*  
doi:10.1093/nar/gkm234
- Kim, H., Reddoch, J. F., Mayfield, C., Ebbinghaus, S., Vigneswaran, N., Thomas, S., . . . Miller, D. M. (1998). Inhibition of transcription of the human c-myc protooncogene by intermolecular triplex . *Biochemistry*, 37(8), 2299-2304.  
doi:10.1021/bi9718191
- Knauert, M. P., & Glazer, P. M. (2001a). Triplex forming oligonucleotides: Sequence-specific tools for gene targeting. *Human Molecular Genetics*, 10(20), 2243.
- Knauert, M. P., & Glazer, P. M. (2001b). Triplex forming oligonucleotides: Sequence-specific tools for gene targeting. *Human Molecular Genetics*, 10(20), 2243-2251.  
doi:10.1093/hmg/10.20.2243
- Kola, I., & Sumarsono, S. (1995). Microinjection of in vitro transcribed RNA and antisense oligonucleotides in mouse oocytes and early embryos to study the gain-and loss-of-function of genes. In M. Tymms (Ed.), (pp. 135-149) Humana Press.  
doi:10.1385/0-89603-288-4:135
- Krawczyk, S. H., Milligan, J. F., Wadwani, S., Moulds, C., Froehler, B. C., & Matteucci, M. D. (1992). Oligonucleotide-mediated triple helix formation using an N3-



protonated deoxycytidine analog exhibiting pH-independent binding within the physiological range. *Proceedings of the National Academy of Sciences*, 89(9), 3761-3764. doi:10.1073/pnas.89.9.3761

Lacoste, J., François, J., & Hélène, C. (1997). Triple helix formation with purine-rich phosphorothioate-containing oligonucleotides covalently linked to an acridine derivative. *Nucleic Acids Research*, 25(10), 1991-1998. doi:10.1093/nar/25.10.1991

Le Naour, F., Rubinstein, E., Jasmin, C., Prenant, M., & Boucheix, C. (2000). Severely reduced female fertility in CD9-deficient mice. *Science*, 287(5451), 319-321. doi:10.1126/science.287.5451.319

Levy, S., & Shoham, T. (2005). Protein-protein interactions in the tetraspanin web. *Physiology*, 20(4), 218-224. doi:10.1152/physiol.00015.2005

Levy-Nissenbaum, E., Radovic-Moreno, A. F., Wang, A. Z., Langer, R., & Farokhzad, O. C. (2008). Nanotechnology and aptamers: Applications in drug delivery. *Trends in Biotechnology*, 26(8), 442-449. doi:<http://dx.doi.org/10.1016/j.tibtech.2008.04.006>

Li, Y., Hou, Y., Ma, W., Yuan, J., Zhang, D., Sun, Q., & Wang, W. (2004). Localization of CD9 in pig oocytes and its effects on sperm-egg interaction. *Reproduction*, 127(2), 151-157. doi:10.1530/rep.1.00006

Lincoln, A. J., Wickramasinghe, D., Stein, P., Schultz, R. M., Palko, M. E., Maria P. De De Miguel, . . . Donovan, P. J. (2002). Cdc25b phosphatase is required for

resumption of meiosis during oocyte maturation. *Nature Genetics*, 30(4), 446-9.  
doi:<http://dx.doi.org/10.1038/ng856>

Lindqvist, A., Källström, H., & Karlsson Rosenthal, C. (2004). Characterisation of Cdc25B localisation and nuclear export during the cell cycle and in response to stress. *Journal of Cell Science*, 117(21), 4979-4990. doi:10.1242/jcs.01395

Livak, K. J., & Schmittgen, T. D. (2001). Analysis of relative gene expression data using real-time quantitative PCR and the 2- $\Delta\Delta$ CT method. *Methods*, 25(4), 402-408.  
doi:10.1006/meth.2001.1262

Lu, L., Wood, J. L., Minter-Dykhouse, K., Ye, L., Saunders, T. L., Yu, X., & Chen, J. (2008). Polo-like kinase 1 is essential for early embryonic development and tumor suppression. *Molecular and Cellular Biology*, 28(22), 6870-6876.  
doi:10.1128/MCB.00392-08

Mahato, R. I., Cheng, K., & Guntaka, R. V. (2005). Modulation of gene expression by antisense and antigene oligodeoxynucleotides and small interfering RNA. *Expert Opinion on Drug Delivery*, 2(1), 3-28. doi:10.1517/17425247.2.1.3

Maher, L., Wold, B., & Dervan, P. (1989). Inhibition of DNA binding proteins by oligonucleotide-directed triple helix formation. *Science*, 245(4919), 725-730.  
doi:10.1126/science.2549631

- Malik, R., & Svoboda, P. (2012). Transgenic RNAi in mouse oocytes: The first decade. *Animal Reproduction Science*, 134(1–2), 64-68.  
doi:10.1016/j.anireprosci.2012.08.012
- Malone, R. W., Felgner, P. L., & Verma, I. M. (1989). Cationic liposome-mediated RNA transfection. *Proceedings of the National Academy of Sciences*, 86(16), 6077-6081.
- McNamara, J. O., Andrechek, E. R., Wang, Y., Viles, K. D., Rempel, R. E., Gilboa, E., . . . Giangrande, P. H. (2006). Cell type-specific delivery of siRNAs with aptamer-siRNA chimeras. *Nat Biotech*, 24(8), 1005-1015.
- Miller, B. J., Georges-Labouesse, E., Primakoff, P., & Myles, D. G. (2000). Normal fertilization occurs with eggs lacking the integrin  $\alpha 6\beta 1$  and is Cd9-dependent. *The Journal of Cell Biology*, 149(6), 1289-1296. doi:10.1083/jcb.149.6.1289
- Miyado, K., Yamada, G., Yamada, S., Hasuwa, H., Nakamura, Y., Ryu, F., . . . Mekada, E. (2000). Requirement of CD9 on the egg plasma membrane for fertilization. *Science*, 287(5451), 321-324. doi:10.1126/science.287.5451.321
- Morvan, F., Porumb, H., Degols, G., Lefebvre, I., Pompon, A., Sproat, B. S., . . . Imbach, J. L. (1993). Comparative evaluation of seven oligonucleotide analogs as potential antisense agents. *Journal of Medicinal Chemistry*, 36(2), 280-287.  
doi:10.1021/jm00054a013

- Noguchi, A., Furuno, T., Kawaura, C., & Nakanishi, M. (1998). Membrane fusion plays an important role in gene transfection mediated by cationic liposomes. *FEBS Letters*, 433(1–2), 169-173. doi:10.1016/S0014-5793(98)00837-0
- Nolan, T., Hands, R. E., & Bustin, S. A. (2006). Quantification of mRNA using real-time RT-PCR. *Nat. Protocols*, 1(3), 1559-1582.
- Pahlavan, G., Polanski, Z., Kalab, P., Golsteyn, R., Nigg, E. A., & Maro, B. (2000). Characterization of polo-like kinase 1 during meiotic maturation of the mouse oocyte. *Developmental Biology*, 220(2), 392-400. doi:10.1006/dbio.2000.9656
- Pal, S. K., Zinkel, S. S., Kiessling, A. A., & Cooper, G. M. (1991). C-mos expression in mouse oocytes is controlled by initiator-related sequences immediately downstream of the transcription initiation site. *Molecular and Cellular Biology*, 11(10), 5190-5196. doi:10.1128/MCB.11.10.5190
- Postel, E. H., Flint, S. J., Kessler, D. J., & Hogan, M. E. (1991). Evidence that a triplex-forming oligodeoxyribonucleotide binds to the c-myc promoter in HeLa cells, thereby reducing c-myc mRNA levels. *Proceedings of the National Academy of Sciences of the United States of America*, 88(18), 8227-8231.
- Povsic, T. J., & Dervan, P. B. (1989). Triple helix formation by oligonucleotides on DNA extended to the physiological pH range. *Journal of the American Chemical Society*, 111(8), 3059-3061. doi:10.1021/ja00190a047

**qPCR efficiency calculator**. Retrieved May/20, 2013, from

<http://www.thermoscientificbio.com/webtools/qpcrefficiency/>

Raaijmakers, M. H. G. P., van Emst, L., de Witte, T., Mensink, E., & Raymakers, R. A.

P. (2002). Quantitative assessment of gene expression in highly purified hematopoietic cells using real-time reverse transcriptase polymerase chain reaction [Abstract]. *Experimental Hematology*, 30(5) 481-487.

Radhakrishnan, I., & Patel, D. J. (1994). DNA triplexes: Solution structures, hydration sites, energetics, interactions, and function. *Biochemistry*, 33(38), 11405-11416.

doi:10.1021/bi00204a001

Radonić, A., Thulke, S., Mackay, I. M., Landt, O., Siegert, W., & Nitsche, A. (2004).

Guideline to reference gene selection for quantitative real-time PCR. *Biochemical and Biophysical Research Communications*, 313(4), 856-862.

doi:10.1016/j.bbrc.2003.11.177

Richards, W. G., Carroll, P. M., Kinloch, R. A., Wassarman, P. M., & Strickland, S.

(1993). Creating maternal effect mutations in transgenic mice: Antisense inhibition of an oocyte gene product. *Developmental Biology*, 160(2), 543-553.

doi:10.1006/dbio.1993.1328

Sandström, K., Wärmländer, S., Gräslund, A., & Leijon, M. (2002). A-tract DNA disfavors triplex formation. *Journal of Molecular Biology*, 315(4), 737-748.

doi:<http://dx.doi.org/10.1006/jmbi.2001.5249>

- Sarnova, L., Malik, R., Sedlacek, R., & Svoboda, P. (2010). Shortcomings of short hairpin RNA-based transgenic RNA interference in mouse oocytes. *Journal of Negative Results in BioMedicine*, 9(1), 1-10. doi:10.1186/1477-5751-9-8
- Sen, A., & Caiazza, F. (2013). Oocyte maturation: A story of arrest and release. *Front Biosci (Schol Ed)*, 5, 451-477.
- Shi, W., Alajez, N. M., Bastianutto, C., Hui, A. B. Y., Mocanu, J. D., Ito, E., . . . Liu, F. (2010). Significance of Plk1 regulation by miR-100 in human nasopharyngeal cancer. *International Journal of Cancer*, 126(9), 2036-2048. doi:10.1002/ijc.24880
- Singleton, S. F., & Dervan, P. B. (1992). Influence of pH on the equilibrium association constants for oligodeoxyribonucleotide-directed triple helix formation at single DNA sites. *Biochemistry*, 31(45), 10995-11003. doi:10.1021/bi00160a008
- Sohn, J., Kristjánisdóttir, K., Safi, A., Parker, B., Kiburz, B., & Rudolph, J. (2004). Remote hot spots mediate protein substrate recognition for the Cdc25 phosphatase. *Proceedings of the National Academy of Sciences of the United States of America*, 101(47), 16437-16441. doi:10.1073/pnas.0407663101
- Spandidos, A., Wang, X., Wang, H., & Seed, B. (2010). PrimerBank: A resource of human and mouse PCR primer pairs for gene expression detection and quantification. *Nucleic Acids Research*, 38(suppl 1), D792-D799. doi:10.1093/nar/gkp1005

- Strebhardt, K., & Ullrich, A. (2006). Targeting polo-like kinase 1 for cancer therapy. *Nature Reviews: Cancer*, 6(4), 321-330.  
doi:<http://dx.doi.org.proxy1.library.jhu.edu/10.1038/nrc1841>
- Takai, N., Hamanaka, R., Yoshimatsu, J., & Miyakawa, I. (2005). Polo-like kinases (plks) and cancer. *Oncogene*, 24(2), 287-291. doi:10.1038/sj.onc.1208272
- Tong, C., Fan, H., Lian, L., Li, S., Chen, D., Schatten, H., & Sun, Q. (2002). Polo-like kinase-1 is a pivotal regulator of microtubule assembly during mouse oocyte meiotic maturation, fertilization, and early embryonic mitosis. *Biology of Reproduction*, 67(2), 546-554. doi:10.1095/biolreprod67.2.546
- Tong, Z., Nelson, L. M., & Dean, J. (1995). Inhibition of zona pellucida gene expression by antisense oligonucleotides injected into mouse oocytes. *Journal of Biological Chemistry*, 270(2), 849-853. doi:10.1074/jbc.270.2.849
- Torgasheva, A., Rubtsov, N., & Borodin, P. (2013). Recombination and synaptic adjustment in oocytes of mice heterozygous for a large paracentric inversion. *Chromosome Research*, 21(1), 37-48. doi:10.1007/s10577-012-9336-6
- Vasquez, K. M., Narayanan, L., & Glazer, P. M. (2000). Specific mutations induced by triplex-forming oligonucleotides in mice. *Science*, 290(5491), 530-533.
- Wang, G., Levy, D. D., Seidman, M. M., & Glazer, P. M. (1995). Targeted mutagenesis in mammalian cells mediated by intracellular triple helix formation. *Molecular and Cellular Biology*, 15(3), 1759-1768.

- Wang, G., Seidman, M. M., & Glazer, P. M. (1996). Mutagenesis in mammalian cells induced by triple helix formation and transcription-coupled repair. *Science*, 271(5250), 802-805.
- Watanabe, N., Arai, H., Nishihara, Y., Taniguchi, M., Watanabe, N., Hunter, T., . . . Ruderman, J. V. (2004). M-phase kinases induce phospho-dependent ubiquitination of somatic Wee1 by SCF $\beta$  - TrCP. *Proceedings of the National Academy of Sciences of the United States of America*, 101(13), 4419-4424.
- Woods, A., & Couchman, J. R. (2000). Integrin modulation by lateral association. *Journal of Biological Chemistry*, 275(32), 24233-24236.  
doi:10.1074/jbc.R000001200
- Wrobel, I., & Collins, D. (1995). Fusion of cationic liposomes with mammalian cells occurs after endocytosis. *Biochimica Et Biophysica Acta (BBA) - Biomembranes*, 1235(2), 296-304. doi:10.1016/0005-2736(95)80017-A
- Wu, Q., Gaddis, S. S., MacLeod, M. C., Walborg, E. F., Thames, H. D., DiGiovanni, J., & Vasquez, K. M. (2007). High-affinity triplex-forming oligonucleotide target sequences in mammalian genomes. *Molecular Carcinogenesis*, 46(1), 15-23.  
doi:10.1002/mc.20261
- Xodo, L. E., Manzini, G., Quadrioglio, F., van der Marel, G. A., & van Boom, J. H. (1991). Effect of 5-methylcytosine on the stability of triple-stranded DNA—a



thermodynamic study. *Nucleic Acids Research*, 19(20), 5625-5631.

doi:10.1093/nar/19.20.5625

Young, S. L., Krawczyk, S. H., Matteucci, M. D., & Toole, J. J. (1991). Triple helix formation inhibits transcription elongation in vitro. *Proceedings of the National Academy of Sciences*, 88(22), 10023-10026.

Zabner, J., Fasbender, A. J., Moninger, T., Poellinger, K. A., & Welsh, M. J. (1995). Cellular and molecular barriers to gene transfer by a cationic lipid. *Journal of Biological Chemistry*, 270(32), 18997-19007. doi:10.1074/jbc.270.32.18997

Zhong, H., & Simons, J. W. (1999). Direct comparison of GAPDH,  $\beta$ -actin, cyclophilin, and 28S rRNA as internal standards for quantifying RNA levels under hypoxia. *Biochemical and Biophysical Research Communications*, 259(3), 523-526.  
doi:10.1006/bbrc.1999.0815

Zhou J FAU - Rossi, John,J., & Rossi, J. J. (0714). *Aptamer-targeted cell-specific RNA interference*

Zhu, G., Miller, B. J., Boucheix, C., Rubinstein, E., Liu, C. C., Hynes, R. O., . . . Primakoff, P. (2002). Residues SFQ (173-175) in the large extracellular loop of CD9 are required for gamete fusion. *Development*, 129(8), 1995-2002.

Benedicta Asamoah

14111 Riverbirch Ct

Laurel, MD

[Beneasam@gmail.com](mailto:Beneasam@gmail.com)

## **EDUCATION**

*Masters of Science – Reproductive and Cancer Biology*

John Hopkins School of Public Health

Anticipated December 2013

Department of Biochemistry and Molecular Biology

Baltimore, MD

*Bachelor of Science - Biological Sciences*

Aug 2006 –Dec 2010

University of Maryland, College Park

## **RESEARCH EXPERIENCE**

*Master's research: Department of Biochemistry and Molecular Science, Johns Hopkins*

*Bloomberg School of Public Health, June 2012-December 2013, (Research Advisers: Dr.*

*Paul Miller and Dr. Janice Evans)*

*Investigating Triplex Forming Oligonucleotides That Target The Mouse Cd9 Gene*

- Identifying, synthesizing and performing biochemical analysis of the properties of Triplex Forming Oligonucleotides (e.g. Phosphoramidites DNA synthesis, HPLC, melts assays, crosslinking assay)

- Substantial in vivo experience in cell biology and molecular techniques such as DNA and RNA isolation, western blotting, Real-time PCR, Reverse Transcriptase-qPCR, immunofluorescence.

*Food and Drug Administration (FDA)/ Joint Institute of Food Safety and Applied Nutrition (JISFAN)*

Internship

Aug 2008 –Jan 2010

- RT-PCR to determine the most cost effective, efficient and timely protocol and instrumentation for DNA and RNA purification
- Mastery of DNA extractions, product isolation, and gel electrophoresis. Assisted in routine ELISA assays, buffer preparation
- Characterized the presence of Salmonella enterica subsp. enterica serovar Enteritidis in Research farm in Virginia using PCR, cloning and DNA sequence analysis tools.

*University of Maryland, College Park at Dr. Borgia's Lab*

Jan 2010 – Dec 2010

Research Assistant (Sexual Selection in Bowerbirds)

- Evolution of mate choice and male display in nonrecourse-based mating systems through analysis of videotaped Satin Bowers in Northern Australia.
- Studied female bowerbirds attraction to finely crafted stick structures (Bowers) built by their male counterparts
- Studied male sexual display and female responsiveness

## **PUBLICATIONS**

- Rump, LV., Asamoah, B., Gonzalez-Escalona, N. 2010. Comparison of commercial RNA extraction kits for preparation of DNA-free total RNA from Salmonella cells. BMC Research Notes. 3:211.  
<http://www.biomedcentral.com/1756-0500/3/211>

